

AD-754 889

WIND TUNNEL MEASUREMENT OF AIRBORNE
TOWED CABLE DRAG COEFFICIENTS

Burdette James Barnes, Jr., et al

Air Force Institute of Technology
Wright-Patterson Air Force Base, Ohio

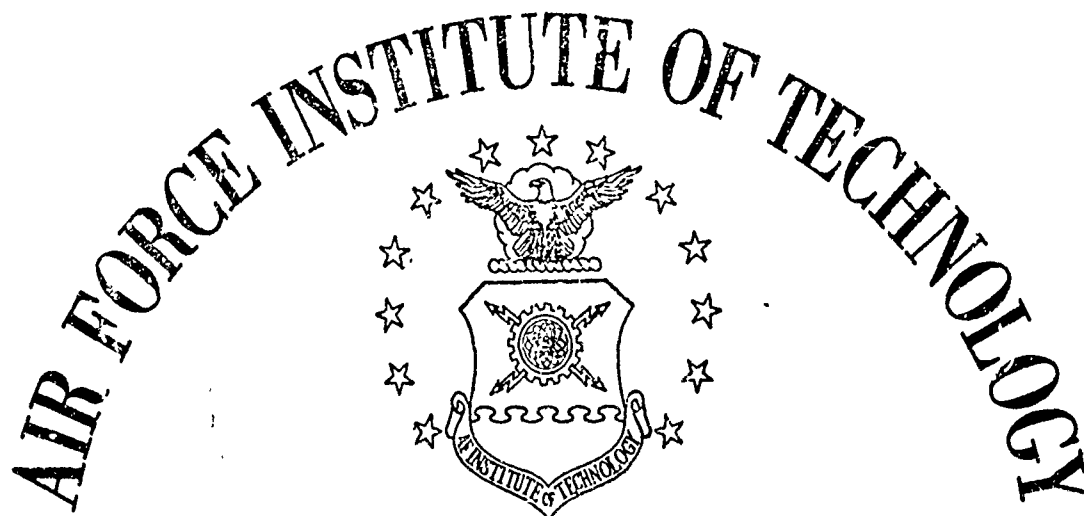
June 1971

DISTRIBUTED BY:

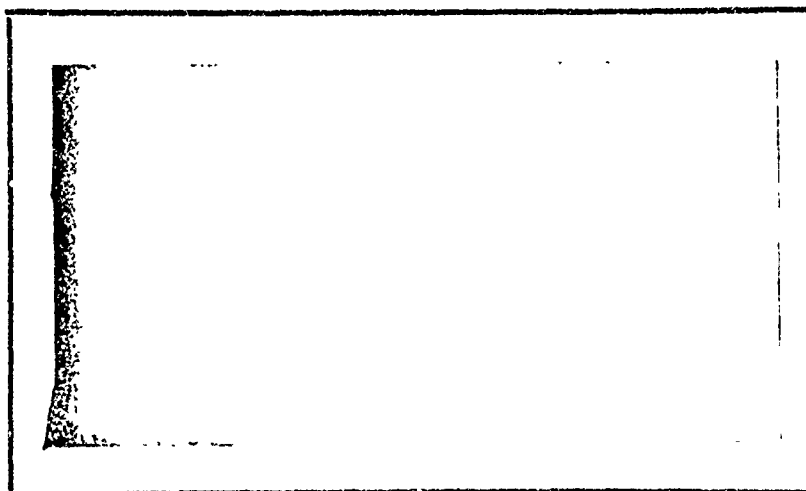
NTIS

National Technical Information Service
U. S. DEPARTMENT OF COMMERCE
5285 Port Royal Road, Springfield Va. 22151

10754389



AIR UNIVERSITY
UNITED STATES AIR FORCE



SCHOOL OF ENGINEERING

Reproduced by
NATIONAL TECHNICAL
INFORMATION SERVICE
U S Department of Commerce
Springfield VA 22151

WRIGHT-PATTERSON AIR FORCE BASE, OHIO

WIND TUNNEL MEASUREMENT OF AIRBORNE
TOWED CABLE DRAG COEFFICIENTS

THESIS

GA/MC/71-4

Burdette J. Barnes, Jr.
Captain USAF

John L. Pothier
Captain USAF

Approved for public release; distribution unlimited.

Unclassified

DOCUMENT CONTROL DATA - R & D

See also the name of title, body of abstract and indexing annotation must be entered when the overall report is classified

Air Force Institute of Technology (AFIT-EN)
Wright-Patterson AFB, Ohio 45433

Unclassified

WIND TUNNEL MEASUREMENT OF AIRBORNE TOWED CABLE DRAG COEFFICIENTS

1. SUMMARY NOTES (Type of report and inclusive dates)

AFIT Thesis

2. AUTHOR(S) (First name, middle initial, last name)

Burdette J. Barnes, Jr. and John L. Pothier
Capt USAF Capt USAF

3. REPORT DATE

June 1971

7a. TOTAL NO OF PAGES

59

7b. NO OF REFS

5

8a. CONTRACT OR GRANT NO

b. PROJECT NO

N/A

9a. ORIGINATOR'S REPORT NUMBER(S)

GA/MC/71-4

9b. OTHER REPORT NO(S) (Any other numbers that may be assigned this report)

10. DISTRIBUTION STATEMENT

Approved for public release; distribution unlimited.

11. SUPPLEMENTARY NOTES

12. SPONSORING MILITARY ACTIVITY

AFIT/GA/MC

13. ABSTRACT Four tow cables used in the AMRL Long Line Loiter program were tested to determine their drag characteristics. Each cable was tested in angle of attack range $\alpha = 15^\circ$ - 90° and Reynolds number range $R_n = 12,000$ - $54,000$. Tests were performed in the AFIT five-foot subsonic wind tunnel. The cables were of two types: (1) two circular, hollow-woven polypropylene lines, for which C_d vs. R_n was generally concave up for high α and nearly linear for the low α . Maximum C_d at $\alpha = 90^\circ$ was near 1.2; the critical R_n was approximately 35,000. (2) two flat ($t/c = 1/2$) hollow-woven nylon lines for which C_d vs. R_n was concave down for high α and nearly linear for low α . Maximum C_d at $\alpha = 90^\circ$ was near 1.0; no critical Reynolds number was reached during flat cable testing.

DD FORM 1473

Unclassified
Security Classification

WIND TUNNEL MEASUREMENT OF AIRBORNE
TOWED CABLE DRAG COEFFICIENTS

THESIS

Presented to the Faculty of the School of Engineering
of the Air Force Institute of Technology
Air University
in Partial Fulfillment of the
Requirements for the Degree of
Master of Science

by

Burdette J. Barnes, Jr., B.S.A.E.
Captain USAF

and

John L. Pothier, B.S.A.E.
Captain USAF

Graduate Astronautical Engineering

June 1971

Approved for public release; distribution unlimited.

Preface

The project which this thesis describes was undertaken with two goals in mind. First, it was hoped that practical information would be obtained for use in the Aerospace Medical Research Laboratory's Long Line Loiter program. Secondly, we hoped to learn as much as we could about "Shirt-sleeve" practical engineering, as well as the theoretical preliminaries and post-test analysis, required to complete a wind tunnel test program.

How successful we have been in our first objective remains to be seen; as far as the second goal is concerned, we gained more experience in practical problem solving, objective re-evaluation, and sheer exasperation than we had ever dared hope.

We express our sincere appreciation to Mr. R. W. Ashabranner, who did the major fabrication of test equipment, and to Messrs. T. J. Lokai and W. S. Whitt for their assistance in running all the tests. We also thank Mrs. Ida M. Barnes, who typed the rough draft of this paper.

We are especially indebted to Professor H. C. Larsen, Head of the Aerospace Design Department of the Air Force Institute of Technology, for his counsel, guidance, and patience with us as we learned throughout this project.

Burdette J. Barnes, Jr.

John L. Pothier

Contents

Preface	ii
List of Figures	iv
Abstract	vii
I. Introduction	1
Background	1
Purpose	2
II. Test Apparatus	3
Drag Frame	3
Cables	12
III. Test Program	16
Prandtl-Tube Rake Calibration	16
Drag Frame Installation and Checkout	19
Pressure/Velocity Survey	22
Drag Frame Tares	23
Cable Drag	25
IV. Accuracy of Data	27
Dynamic Pressures	27
Drag Forces	27
Data Repeatability	27
V. Results and Conclusions	28
Results	28
Conclusions	37
Summary	38
VI. Recommendations	39
Bibliography	40
Appendix A: Cross Flow Principle	41
Appendix B: Data Reduction	44
Appendix C: Graphical Results of Cable Drag Test Program	46
Vitae	58

List of Figures

<u>Figure</u>		<u>Page</u>
1	Drag Frame Side Plate	4
2	Side Plate Inner Surface	5
3	Cable V-Configuration	7
4	Vertex Pylon	8
5	Drag Frame Front View	9
6	Strain Gauge C-Link	10
7	Adjustable Cable Anchor	11
8	Cables 1 and 2	13
9	Cable 3	14
10	Cable 4	15
11	Prandtl-Tube Rake Installation	17
12	Prandtl Tube Calibration (typical)	18
13	Drag Frame Installed in Test Section (Front View)	19
14	Wire Balance Attachment Points	20
15	Damper/Tether Attachment Points (Left Side)	21
16	Cable Test Volume	22
17	Drag Frame Tares as a Function of Test Section Dynamic Pressure	24
18	Cable Angle of Attack	25
19	Cable 1: Coefficient of Drag as a Function of Reynolds Number, Angle of Attack as Parameter (25 lb tension)	29
20	Cable 1: Coefficient of Drag as a Function of Angle of Attack, Reynolds Number as Parameter (25 lb tension)	30

<u>Figure</u>		<u>Page</u>
21	Cable 1: Comparison of Predicted and Measured Variation of Drag Coefficient with Angle of Attack ($R_n = 37,000$, 25 lb tension)	31
22	Cable 2: Coefficient of Drag as a Function of Reynolds Number, Angle of Attack and Tension as Parameters	32
23	Cable 3: Coefficient of Drag as a Function of Reynolds Number, Angle of Attack as Parameter (25 lb tension)	34
24	Cable 3: Coefficient of Drag as a Function of Angle of Attack, Reynolds Number as Parameter (25 lb tension)	35
25	Inclined Circular Cylinder in Airstream .	41
26	"Proper" Cross Sectional Area (For a Flat Cable)	45
27	Cable 1: Coefficient of Drag as a Function of Reynolds Number, Angle of Attack as Parameter (25 lb tension)	47
28	Cable 1: Coefficient of Drag as a Function of Angle of Attack, Reynolds Number as Parameter (25 lb tension)	48
29	Cable 1: Comparison of Predicted and Measured Variation of Drag Coefficient with Angle of Attack ($R_n = 37,000$, 25 lb tension)	49
30	Cable 2: Coefficient of Drag as a Function of Reynolds Number, Angle of Attack as Parameter (25 lb tension)	50
31	Cable 2: Coefficient of Drag as a Function Of Reynolds Number, Angle of Attack as Parameter (100 lb tension)	51
32	Cable 2: Coefficient of Drag as a Function of Angle of Attack, Reynolds Number as Parameter (25 lb tension)	52
33	Cable 2: Comparison of Predicted and Measured Variation of Drag Coefficient with Angle of Attack ($R_n = 19,000$, 25 lb tension)	53

<u>Figure</u>		<u>Page</u>
34	Cable 3: Coefficient of Drag as a Function of Reynolds Number, Angle of Attack as Parameter (25 lb tension)	54
35	Cable 3: Coefficient of Drag as a Function of Angle of Attack, Reynolds Number as Parameter (25 lb tension)	55
36	Cable 4: Coefficient of Drag as a Function of Reynolds Number, Angle of Attack as Parameter (25 lb tension)	56
37	Cable 4: Coefficient of Drag as a Function of Angle of Attack, Reynolds Number as Parameter (25 lb tension)	57

Abstract

Four tow cables used in the Aerospace Medical Research Laboratory's Long Line Loiter (circling towed cable) program were tested to determine their drag characteristics. Each cable was tested with 25 pounds tension at angle of attack $\alpha = 15, 30, 45, 60, 75,$ and 90 degrees in a Reynolds number range $Rn = 12,000 - 54,000$ ($45 - 150$ mph). Tests were performed in the AFIT five-foot subsonic wind tunnel.

The four cables were of two types: two circular, hollow-woven polypropylene lines and two flat ($t/c = 1/2$) hollow-woven nylon lines. Plots of drag coefficient C_d versus Rn for the circular lines had a general concave up shape at high α and were nearly linear at low α . At 90 degrees, the circular line maximum C_d was near 1.2 ; the critical Rn was approximately $35,000$. The relation

$$C_d (\alpha \text{ less than } 90^\circ) = C_d (\alpha = 90^\circ) \sin^3 \alpha$$

was found to predict the shape of the C_d versus α curves, but gave lower values than experimental results.

Plots of C_d versus Rn for the flat cables showed a concave down characteristic at high α and were nearly linear at low α . At 90 degrees, the maximum C_d was approximately 1.0 ; no critical Rn was reached during flat cable testing. It was found that the "sine cubed" prediction was very inaccurate for this type tow cable.

WIND TUNNEL MEASUREMENT OF
AIRBORNE TOWED CABLE
DRAG COEFFICIENTS

I. Introduction

Background

The exact equations of motion of a towed cable are second order nonlinear partial differential equations of such complexity that analytic solutions are not possible without making simplifying assumptions. Among the more commonly used simplifications is the representation of the towed cable as a finite number of inflexible links of uniform point mass, constant cross sectional area, and constant surface roughness, each link experiencing aerodynamic forces resulting from the component of local flow normal to each link's axis (Ref 2:8).

In the case of the circling towed cable, an aircraft flies a circular ground track trajectory while towing the cable; the cable descends from the aircraft toward the ground in a spiral, its trailing length becoming gradually more vertical until the free end is stationary over a selected ground point (Ref 5:1).

Due to the wide variations in angle of attack and airflow velocity acting on each link in a circling towed cable, the assumption that only the normal component of local flow has an aerodynamic effect (the Cross Flow

Principle: see Appendix A) is not applicable to all links. Those links at small angles of attack experience comparatively large axial flow components which lead to the formation of axial boundary layers whose effects cannot be ignored. Further, the effects of cable tension, roughness, and porosity on the drag of a specific cable in oblique flow are not known exactly, making accurate prediction of a given cable's drag characteristics impossible.

Purpose

It was the purpose of this thesis to determine through wind tunnel tests the variation of drag coefficient with Reynolds number and angle of attack for four specific cables used in the AMRL Long Line Loiter (circling towed cable) program. The results of the tests were compared with the results predicted by the Cross Flow Principle and previous NACA test data. Also, the qualitative effects of cable tension on drag were examined briefly for one cable. The AFIT Five-Foot Subsonic Wind Tunnel was used in conducting these tests.

II. Test Apparatus

Drag Frame

Because the aerodynamic drag force experienced by a single short length of tow cable in a low-velocity air-stream is small, it was necessary to maximize the forces to be measured during testing. However, since the AFIT wind tunnel is of circular cross section, an auxiliary test cell, the Drag Frame, was designed and built so that four identical cable specimens could be tested simultaneously.

The Drag Frame consisted of two parallel 1/2-inch plywood plates, 32 inches high by 58 inches long, held 18 inches apart by four 1/2-inch by 3-inch streamlined horizontal struts. To prevent longitudinal bowing, the plates were stiffened by 1 1/2-inch by 1 1/2-inch aluminum angles bolted to the plate outer surfaces as shown in Fig. 1. To keep the flow between the plates as stable as possible, the plate leading edges were bevelled and their inner surfaces sanded smooth. See Fig. 2.

Each cable to be tested was positioned in a V-configuration between the side plates, vertex downstream, giving the effect of two cables at the same angle of attack. This arrangement not only allowed rather long lengths of cable to be tested without requiring an extremely long Drag Frame length, but also minimized the effects of lateral flow components. The vertex was formed by passing the cable over a pulley attached to a pylon formed by three 1/2-inch by



Fig. 1. Drag Frame Side Plate



Fig. 2. Side Plate Inner Surface

3-inch streamlined aluminum struts. See Fig. 3. The horizontal pylon struts bore on the upper and lower edges of the side plates, while the vertical strut was held midway between the side plates. The vertex pylon is shown in Fig. 4. The planes of the four cable specimens tested were spaced vertically 6 inches apart, as shown in Fig. 5.

The ends of each cable were passed through small slots in the side plates and around pulleys mounted to the side plate stiffening angles. One cable end was fastened to a strain gauge C-link which was in turn fastened to a stiffening angle (See Fig. 6), while the other cable end was attached to an adjustable anchor on a stiffening angle. See Fig. 7.

The angle of attack of each cable was set by positioning the vertex pylon at different longitudinal stations, keeping the cable ends at the same locations on the side plates. The strain gauge C-links were used to measure the tension in each line; by adjusting each anchor, all cables could be tested at the same tension.

68 WC/71-4

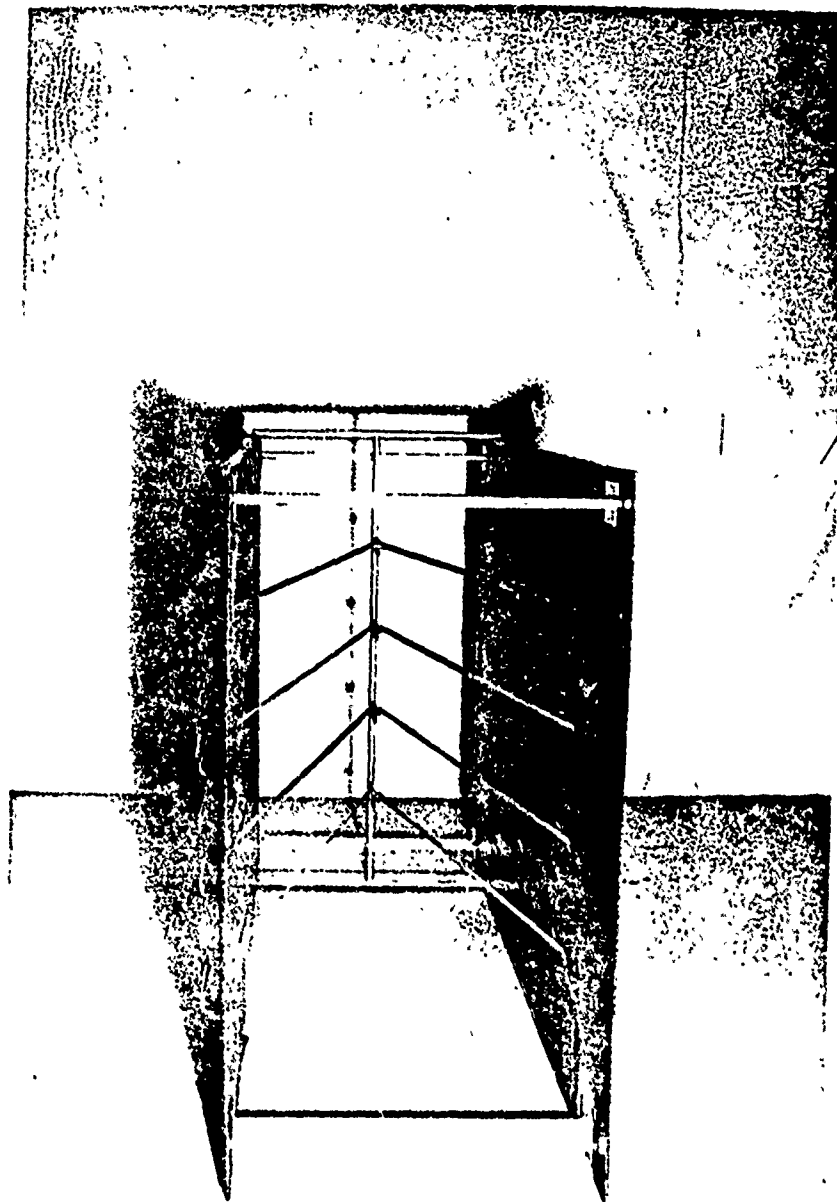


Fig. 3. Cable V-Configuration

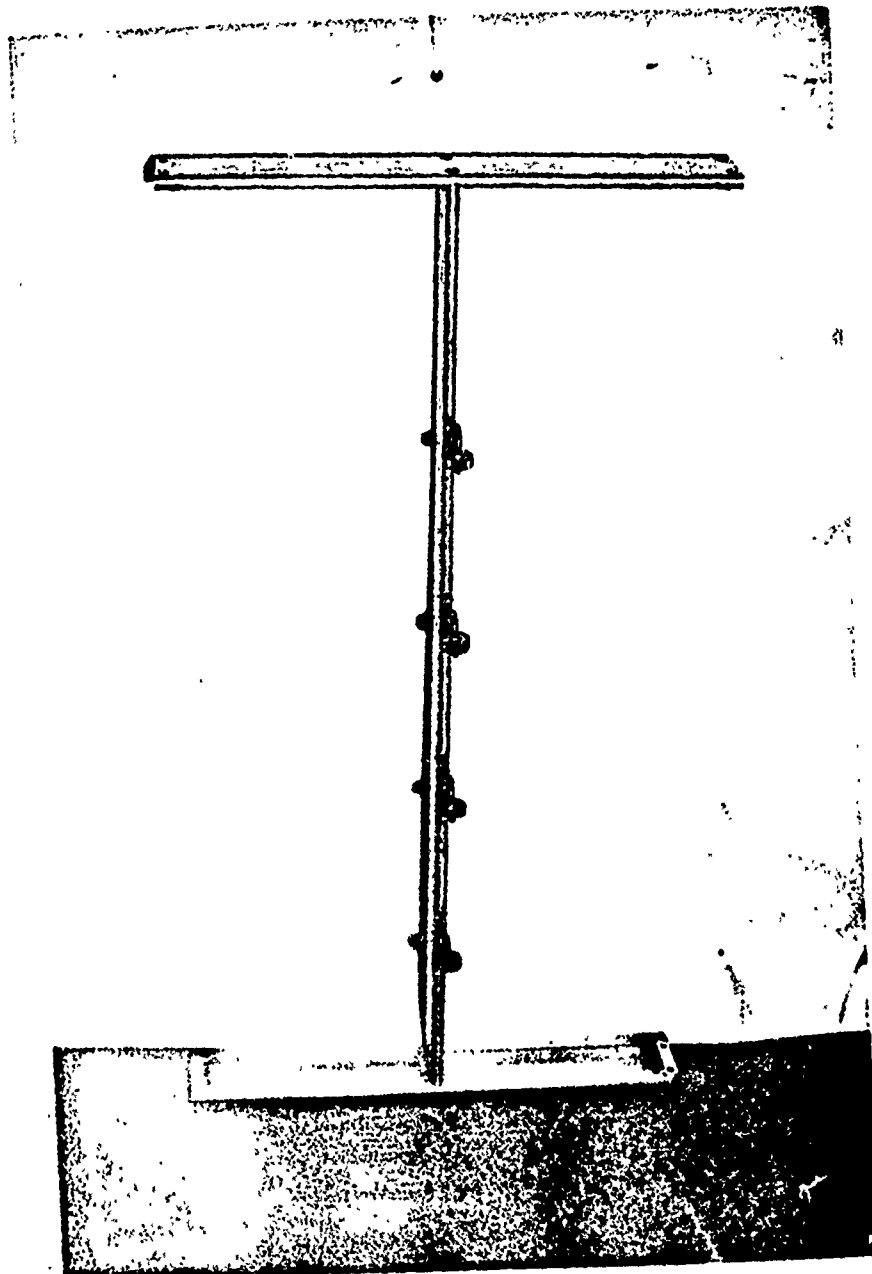


Fig. 4. Vertex Pylon



Fig. 5. Drag Frame Front View

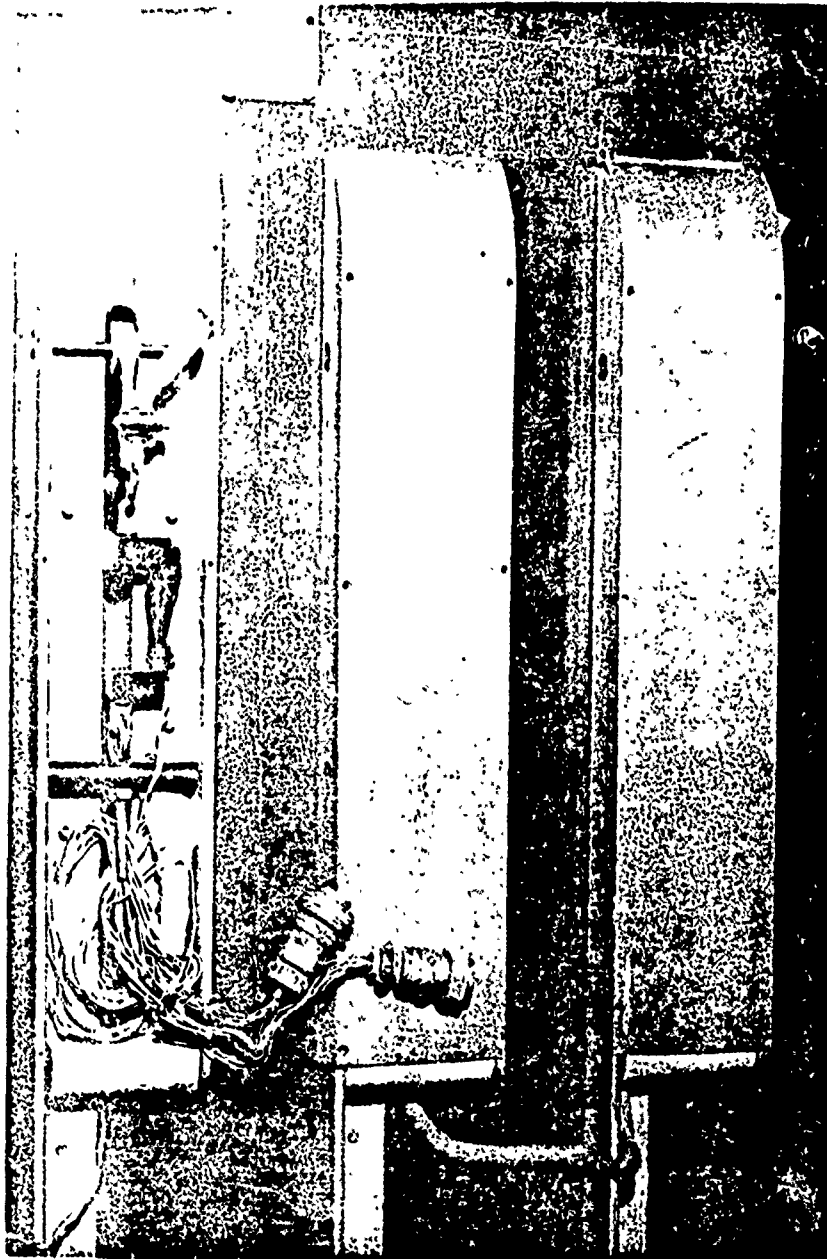


Fig. 6. Strain Gauge C-Link

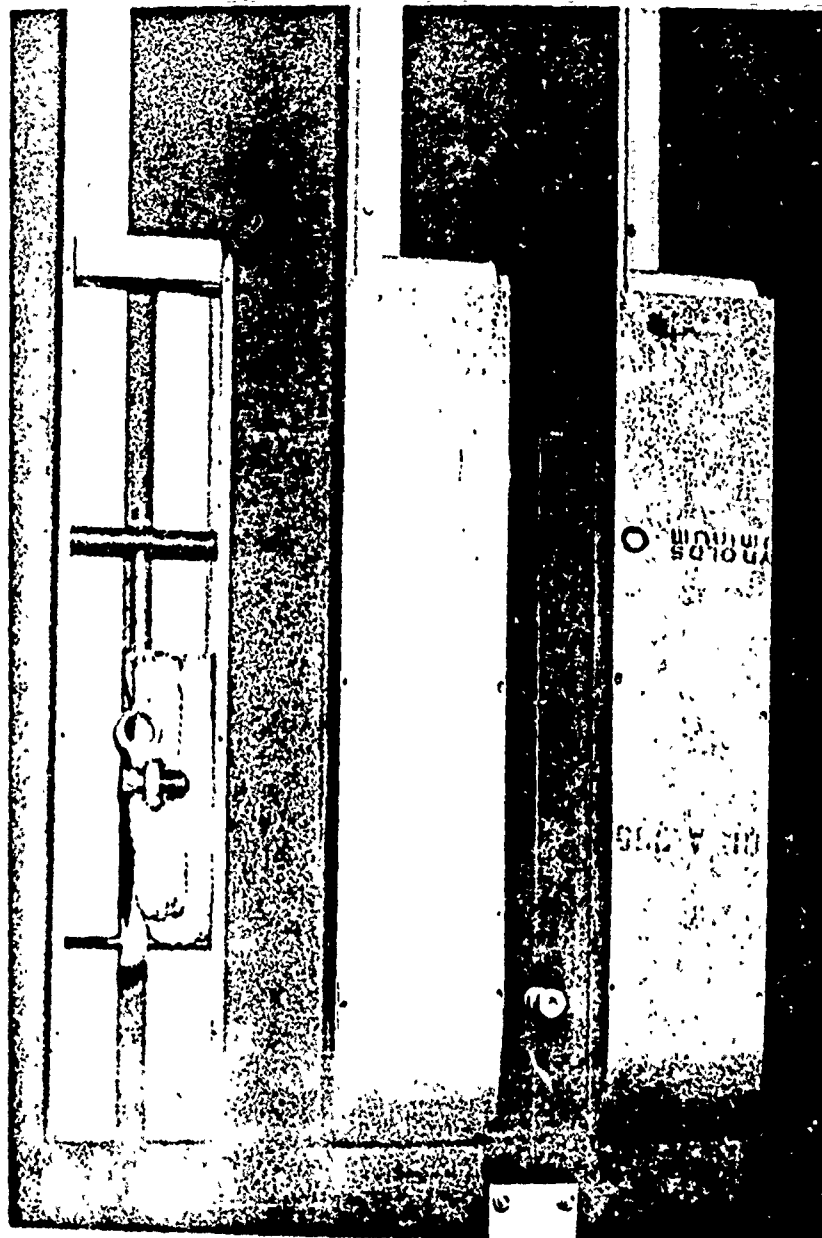


Fig. 7. Adjustable Cable Anchor

Cables

The first cable tested was a hollow-woven polyethylene line of 2000 pounds tensile strength which had a cross sectional diameter of 3/8 inch under 25 pounds tension. This line had a very slick surface, but was essentially rough and porous due to its coarse-woven nature. The second cable was identical to the first, except that four #20 wires were threaded inside the woven exterior. Cable 2 had a 7/16-inch cross sectional diameter under 25 pounds tension and a 3/8-inch diameter under 100 pounds tension. See Fig. 8.

The third cable tested was a hollow-woven nylon line of 4000 pounds tensile strength whose cross section under 25 pounds tension was 1/2 inch by 1/4 inch. This cable was smoother over all than the first and second cables, although its surface finish was much less slick. See Fig. 9.

The fourth cable was very similar to Cable 3, being a hollow-woven nylon line of 2000 pounds tensile strength whose cross section under 25 pounds tension was 3/8 inch by 3/16 inch. Cable 4 was also much less porous and rough than Cables 1 and 2, although not as slick. This cable is shown in Fig. 10.

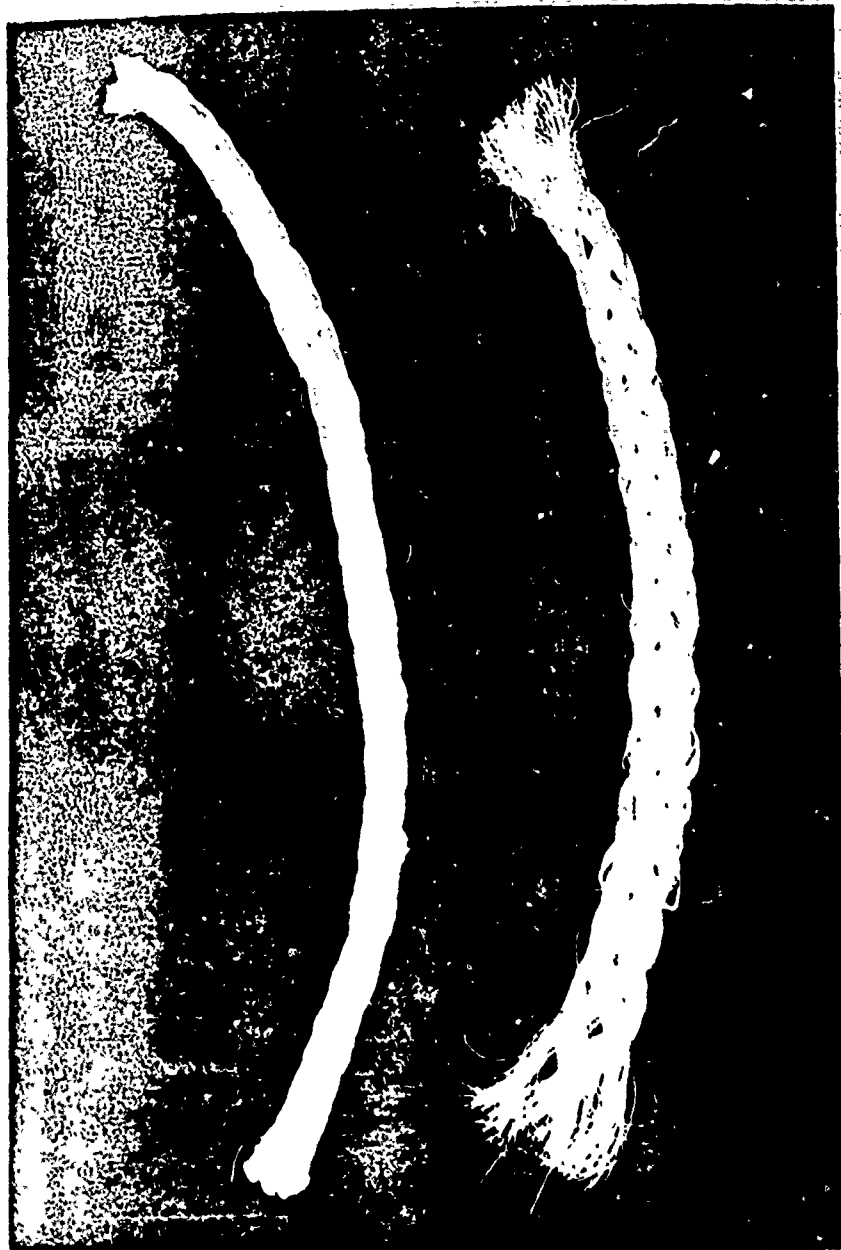


Fig. 8. Cables 1 and 2

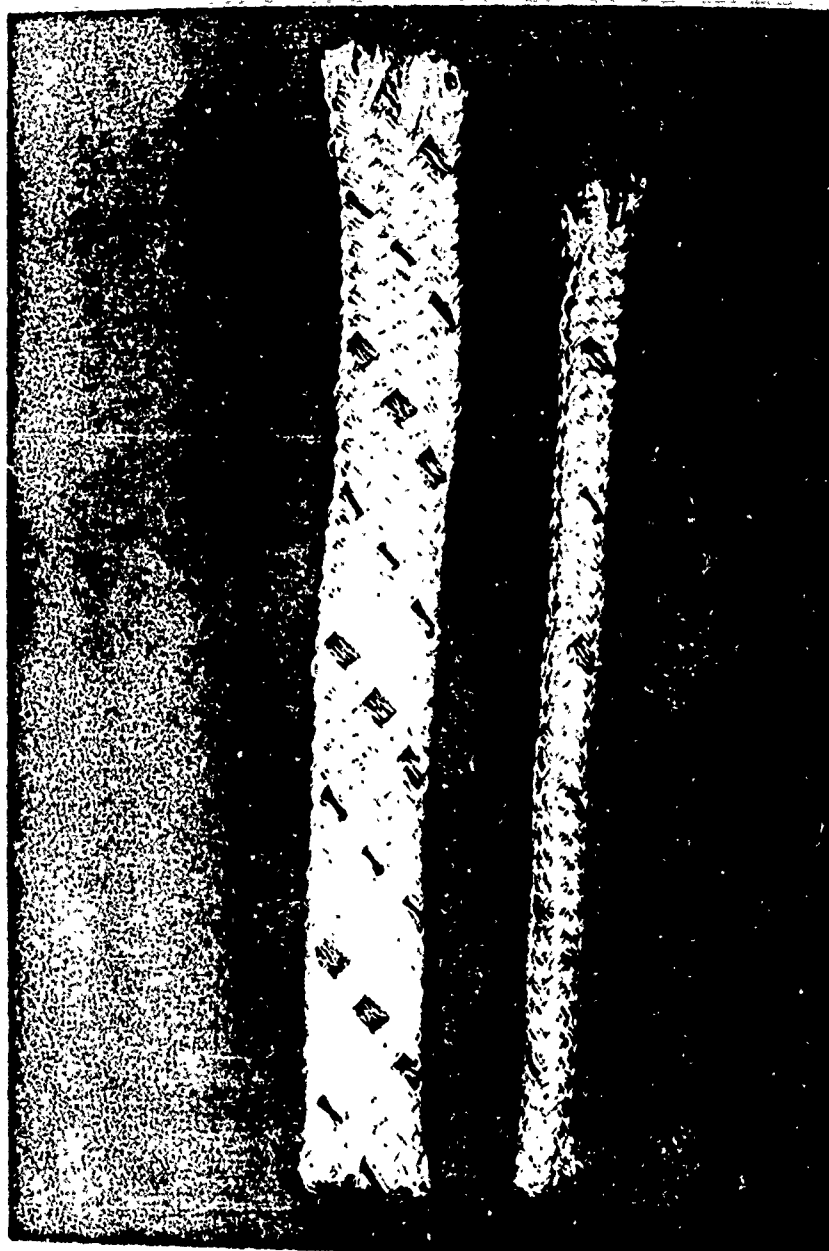


Fig. 9. Cable 3



Fig. 10. Cable 4

III. Test Program

The test program which was followed consisted of five phases:

1. Calibration of the Prandtl-tube pressure rake
2. Installation and checkout of the Drag Frame
3. Pressure/velocity survey of the test volume between the Drag Frame side plates
4. Measurement of Drag Frame drag tares
5. Measurement of cable drag

The descriptions of all test program test phases follow in this section; the general results of Phases 1 through 4 are also presented in this section, while the detailed results of Phase 5, cable drag, are presented in Section V.

Prandtl-Tube Rake Calibration

The four-element Prandtl-tube pressure rake which was used for pressure/velocity surveys was calibrated in the wind tunnel at known tunnel velocities to determine its accuracy. The individual Prandtl tubes were spaced at six inch intervals on the rake, beginning at a point nine inches above the center line and extending to a point nine inches below the center line. The rake was installed in a vertical plane, centered in the tunnel test section, with the tips of the Prandtl tubes 100 inches downstream of the test section entrance, as shown in Fig. 11.

The rake pressure readings were recorded with the rake in the "upright" position; the rake was then inverted and

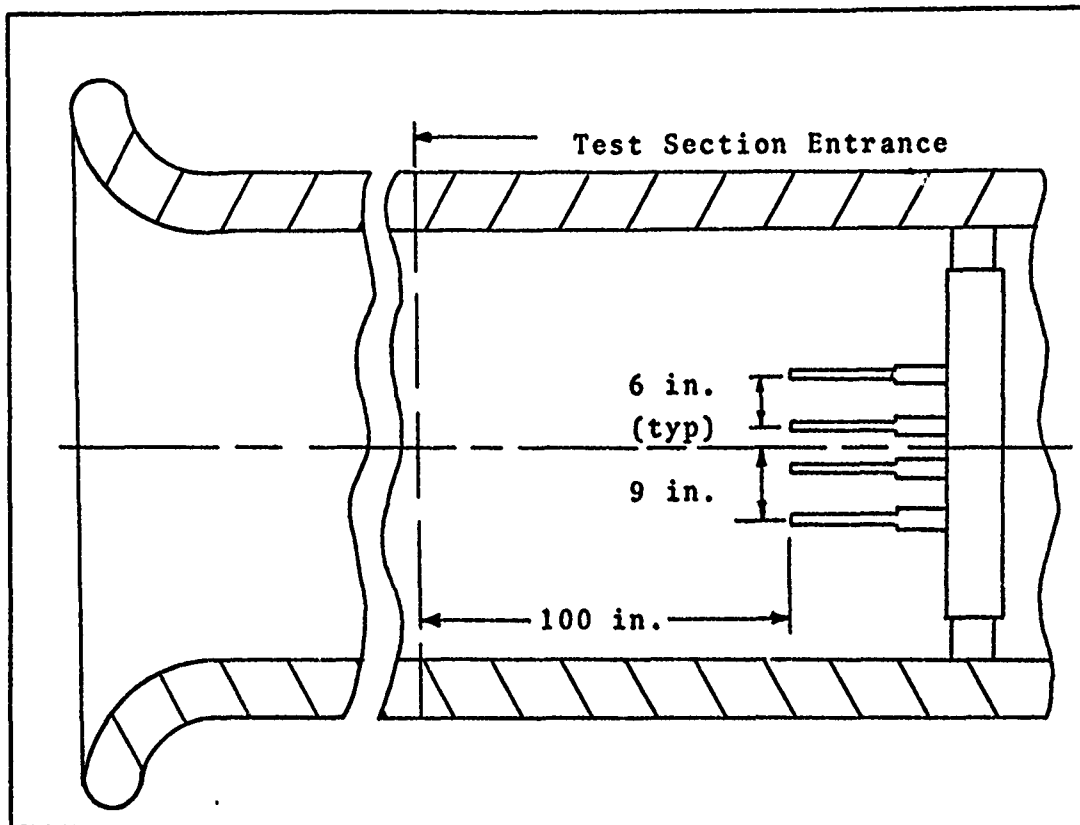


Fig. 11. Prandtl-Tube Rake Installation

pressure readings recorded for the "inverted" position. Analysis of these data indicated that no vertical pressure gradient existed at the chosen calibration location (this was confirmed by previous tunnel pressure survey records) and that all four Prandtl tubes consistently read only 96 per cent of the actual local dynamic pressure. A typical result of Prandtl tube calibration is shown in Fig. 12.

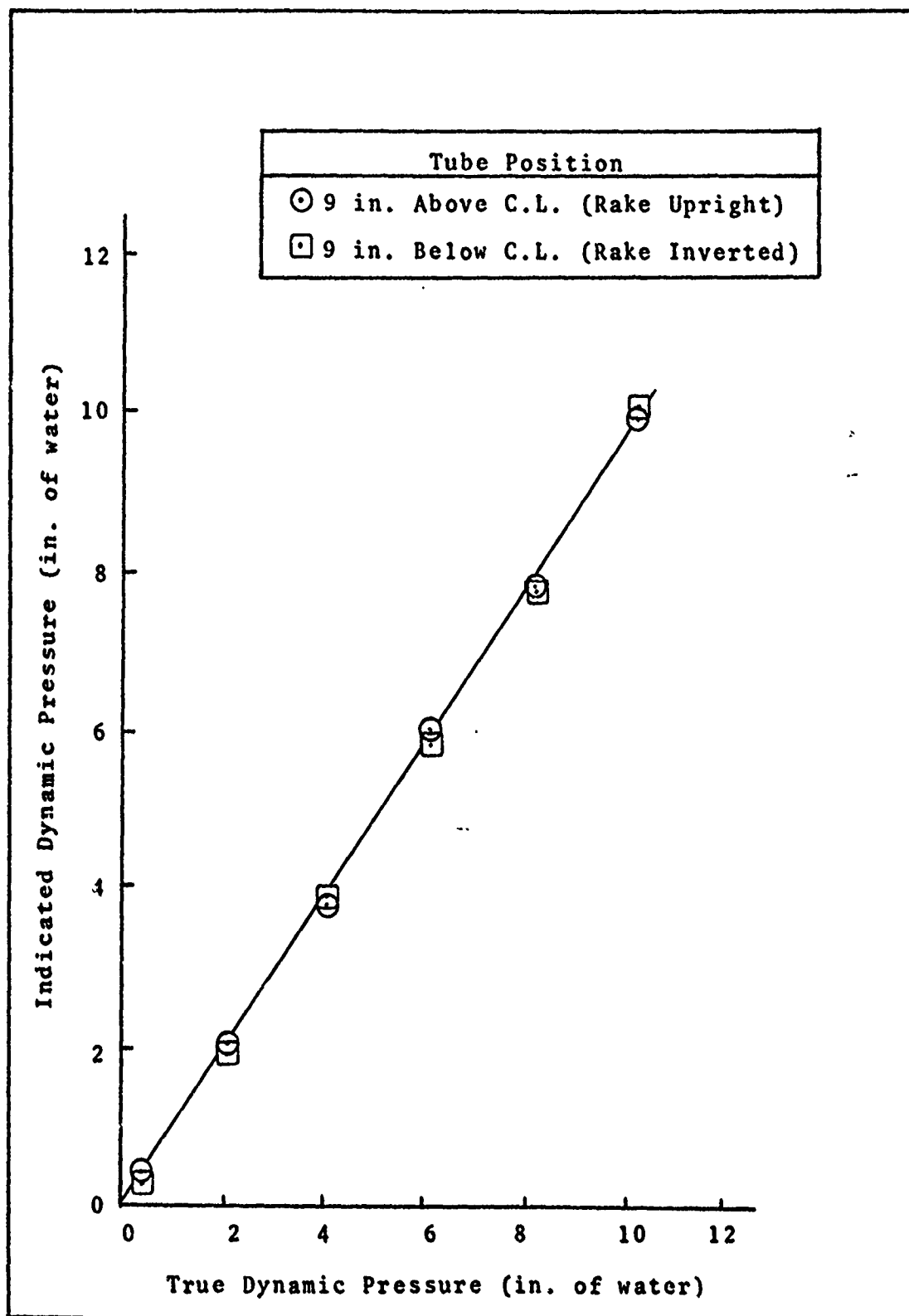


Fig. 12. Prandtl Tube Calibration (typical)

Drag Frame Installation and Checkout

The Drag Frame was installed and attached to the wind tunnel wire balance force measurement system so that it was centered horizontally and vertically in the test section and was at zero angle of attack to the test section longitudinal centerline. A frontal view of the installed Drag Frame is shown in Fig. 13; the wire balance attachment points are shown in Fig. 14.

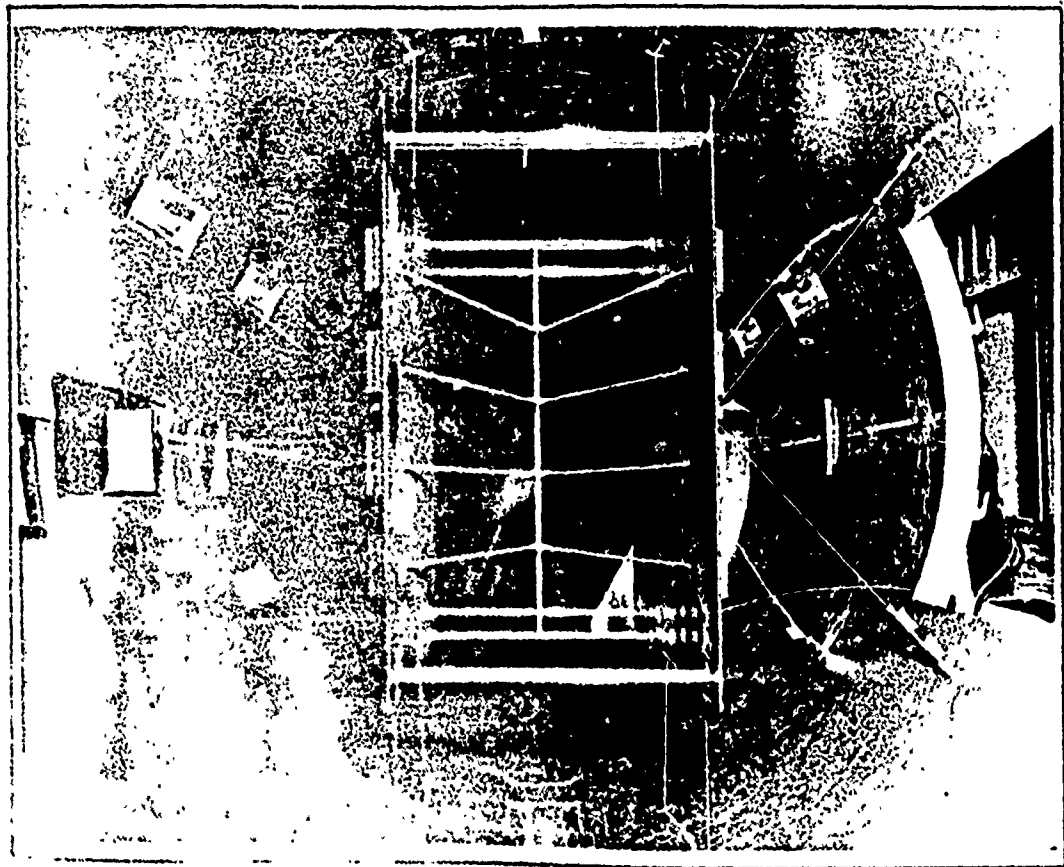


Fig. 13. Drag Frame Installed in Test Section
(Front View)

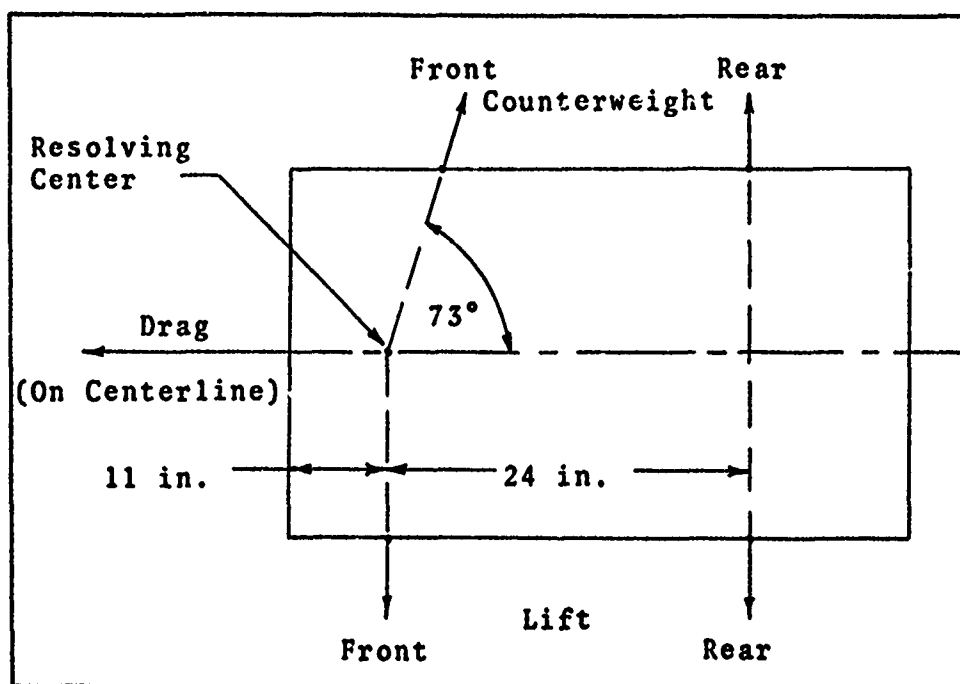


Fig. 14. Wire Balance Attachment Points

From the standpoint of aerodynamic lateral stability, it was desired to have the Drag Frame center of gravity located between the wire balance resolving center (upstream) and the Drag Frame center of pressure (downstream). However, this was not possible because of the location of the center of pressure at approximately the side plate quarter-chord and the center of gravity at approximately mid-chord. The chosen solution to this problem was the use of lateral dampers and tether lines attached to the Drag Frame side plates.

The lines from the viscous dampers were attached to the side plates 12 inches below the resolving center at

the forward position and 36 inches aft of the resolving center on the side plate centerline at the aft position. Tether lines were attached to the left side of the Drag Frame only. The Drag Frame was found to be aerodynamically stable under these constraints throughout the test speed range (0 - 150 mph). The damper and tether line attachment points for the left side plate are shown below in Fig. 15.

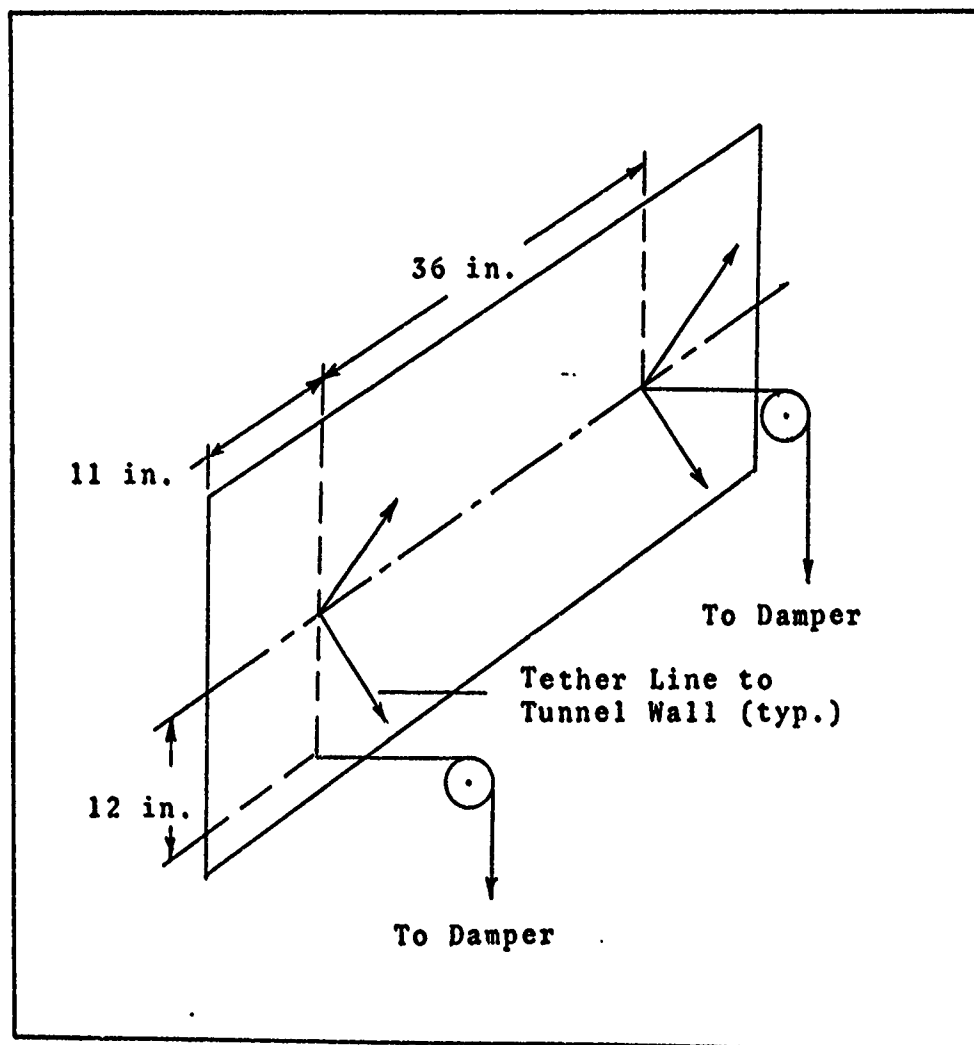


Fig. 15. Damper/Tether Attachment Points
(Left Side)

Pressure/Velocity Survey

All cable test configurations were contained in the volume shown in Fig. 16.

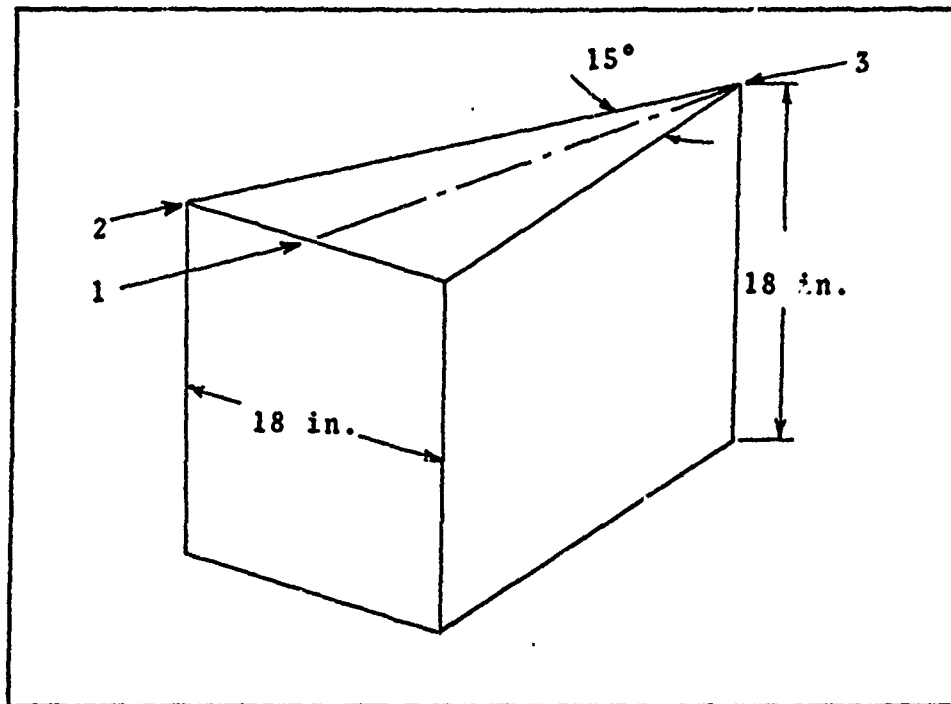


Fig. 16. Cable Test Volume

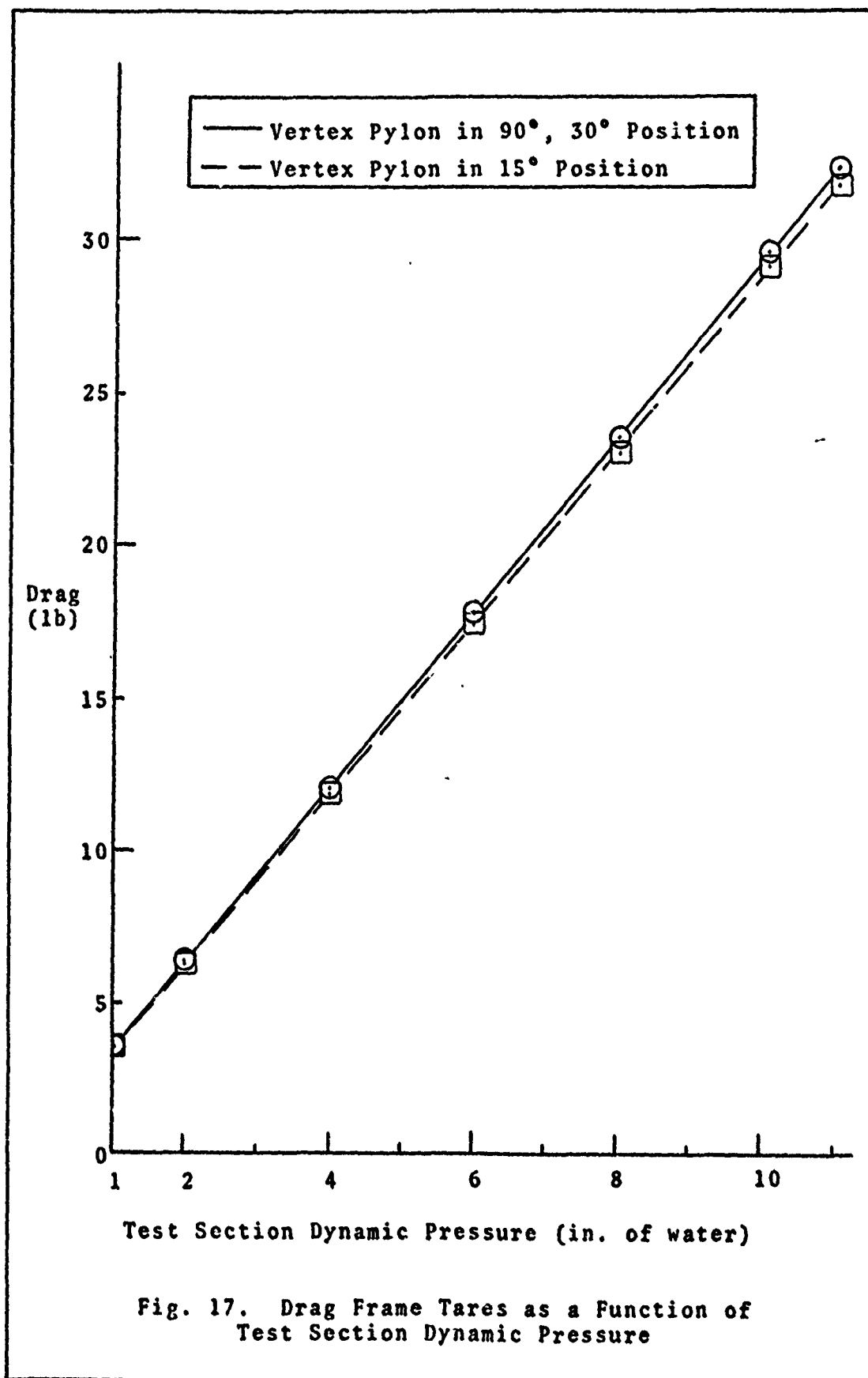
The Prandtl-tube pressure rake was used to survey the pressure/velocity characteristics at Points 1, 2, and 3 in the plane of each cable over the desired tunnel speed range (0 - 150 miles per hour; 0 - 11 inches of water dynamic pressure). It was found that over the entire test pressure range the dynamic pressure at Points 1 and 2 was the same within 0.02 inches of water, while the pressure at Point 3 was approximately 2 per cent higher than at Points 1 and 2. This result was typical of all four cable planes.

By averaging logarithmically the dynamic pressures in all cable planes at Points 1, 2, and 3, an average test

pressure was developed which, over the test range, was within 1 1/2 per cent of the true dynamic pressure at any point within the test volume. Further, this average dynamic pressure was within 1 per cent of the true pressure at Points 1 and 2 in each cable plane. Since only a small portion of the 15 degree angle of attack cables was in the region near Point 3, it was felt that the average test pressure used in computations was within 1 per cent of the true dynamic pressure acting on the cables during test, for all configurations.

Drag Frame Tares

The Drag Frame tares were measured at selected tunnel air speeds with the vertex pylon at the 15, 30, and 90 degree positions. It was found that the 30 and 90 degree vertex pylon configurations gave virtually identical tares, while the 15 degree position resulted in slightly lower tare values. The tares for the 30/90 degree configuration were used for all but the 15 degree angle of attack cable configuration; the 15 degree tare was used for this configuration. Drag Frame tares are plotted versus test section dynamic pressure in Fig. 17.



Cable Drag

All four cables were tested with 25 pounds tension over a test section speed range of approximately 45 to 150 miles per hour (1 - 11 in. of water dynamic pressure) and at 15, 30, 45, 60, 75, and 90 degrees angle of attack. Angle of attack in this test was defined as the angle that the cable center line made with the airstream, as shown below in Fig. 18.

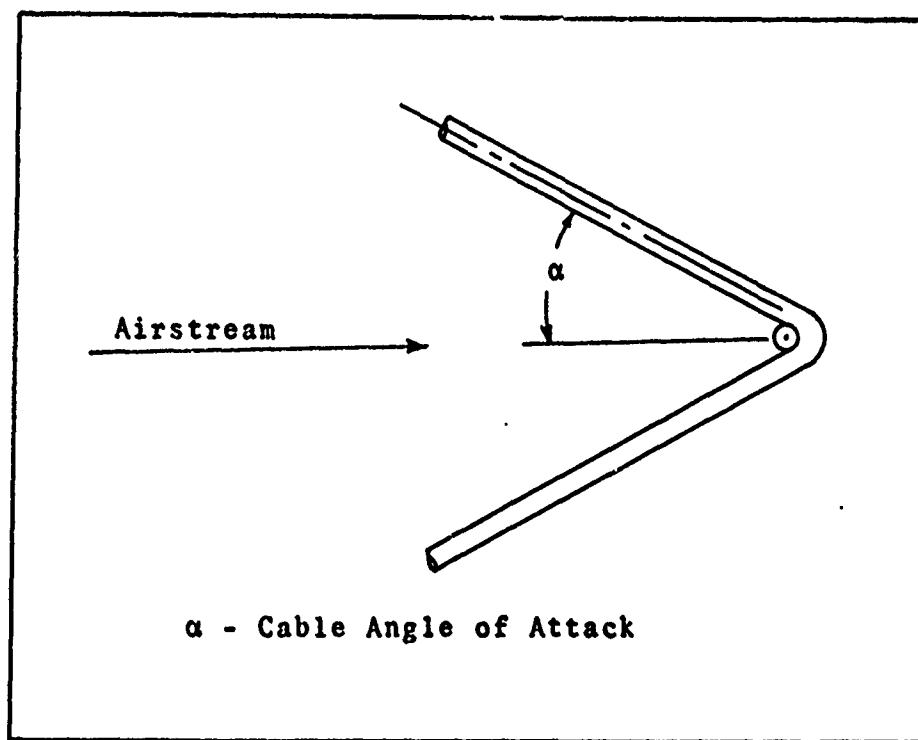


Fig. 18. Cable Angle of Attack

Although a maximum test velocity of 200 miles per hour (corresponding to the usual tow velocity of the C-130 tow aircraft) was desired, this velocity was not attainable due to the excessive wind tunnel motor power required to overcome the high blockage and drag of the Drag Frame.

The lowest test angle of attack, 15 degrees, was chosen so that the length of the Drag Frame which would be required to contain this cable configuration would not be too great.

Cable 2 was also tested with 100 pounds tension at 15, 30, and 45 degrees angle of attack; at 60 degrees, it was apparent that the Drag Frame side plates were bowed inward, making the previously measured drag tares not usable. No measurable side plate bowing occurred during the 25-pound tension tests of any cable.

During testing of the flat cables, Cables 3 and 4, all cable configurations were with the larger cross sectional dimension parallel to the airstream; it was felt that this most closely represented the attitude of a long flat cable during towing.

The results of the cable drag tests are reported in Section V, along with typical graphical results. Graphical results of the complete cable drag test program are presented in Appendix C.

IV. Accuracy of Data

Dynamic Pressures

The nominal tunnel dynamic pressure values for each test point were read on an inclined water manometer having a scale resolution of 0.001 inches of water. However, the dynamic pressure values used for reduction of data resulted from logarithmic averaging of the cable test volume pressure survey data (see Section III, p. 22). The pressure data used in the averaging process were read on a vertical water manometer having a scale resolution of 0.02 inches of water.

Drag Forces

The drag forces which were measured during drag tare and cable drag testing were read on a Toledo beam balance scale having a scale resolution of 0.02 pounds. Three pre-run and three post-run static values were averaged for each cable test; "wind on" forces resulted from averaging five drag force print-outs at each cable/angle of attack/dynamic pressure combination.

Data Repeatability

Due to severe time limitations, it was not possible to conduct a systematic check of data repeatability. However, comparison of C_d versus R_n curves for Cable 2 at 25 and 100 pounds tension and 15, 30, and 45 degrees angle of attack shows good agreement. Also, the general shapes of the curves for Cables 1 and 2 were the same, lending further support to the belief that the data are accurate and could be reproduced.

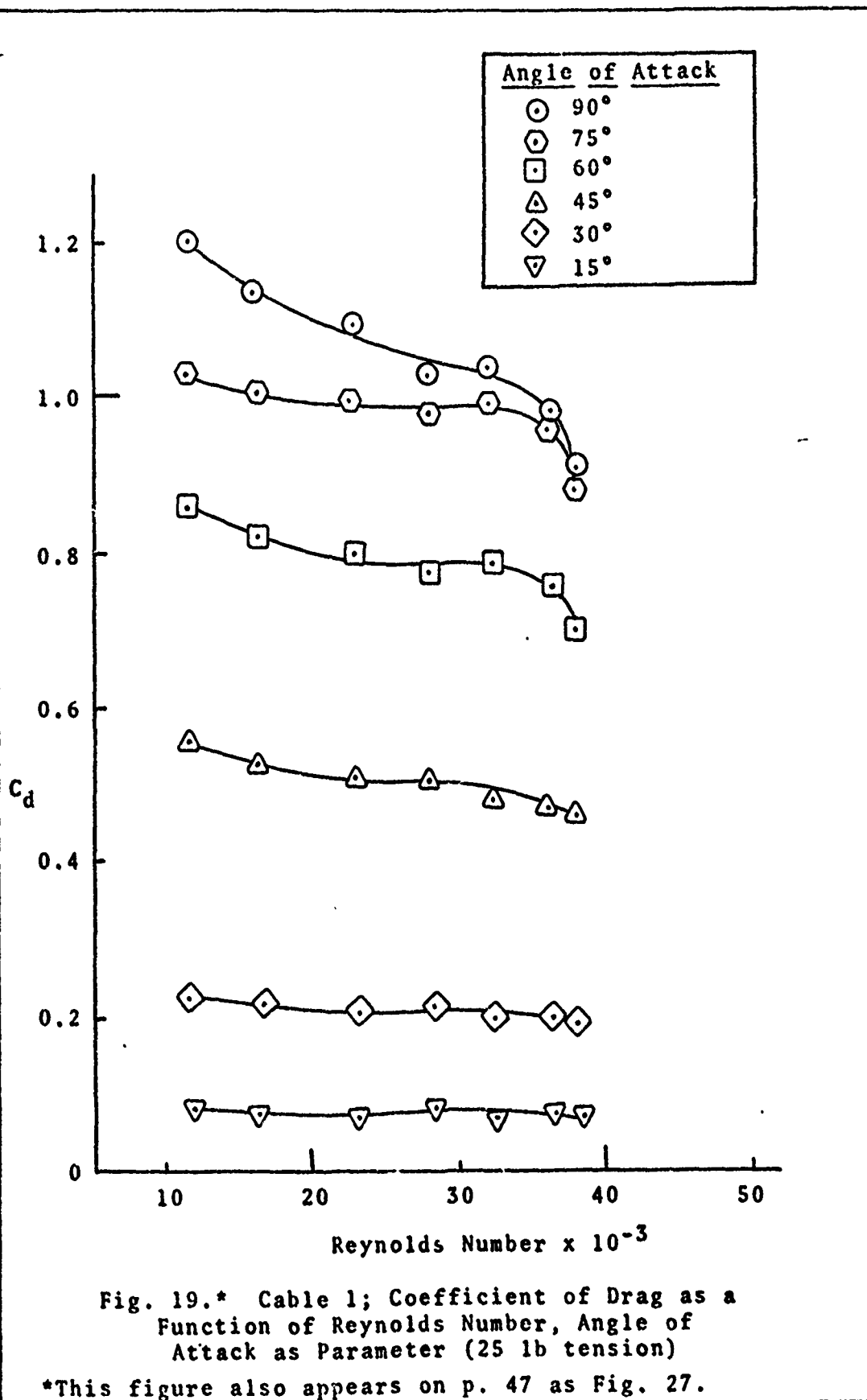
V. Results and ConclusionsResults

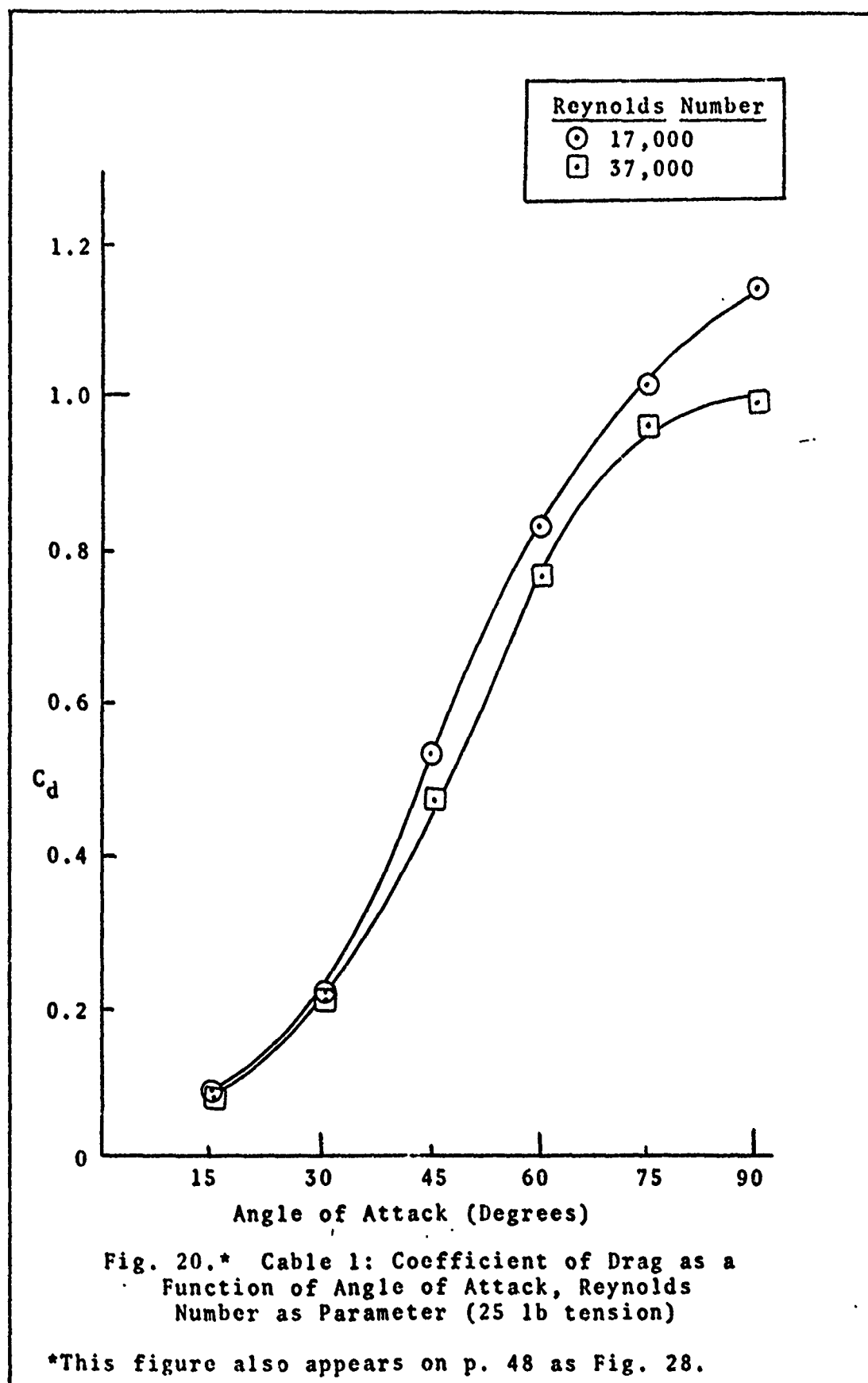
Cable 1. Cable 1 was tested over the Reynolds number range $R_n = 12,000-38,000$. In general, as angle of attack was increased, the coefficient of drag was found to increase, reaching a maximum of 1.2. Also, at a constant angle of attack the coefficient of drag tended to decrease with increasing Reynolds number. At the lower angles of attack, however, this was not as pronounced, and the coefficient of drag was nearly constant at 15 and 30 degree angles of attack. See Fig. 19.

All curves of coefficient of drag versus Reynolds number exhibited a concave upward shape until the critical Reynolds number was reached in the neighborhood of 35,000; at this point there was a sudden decrease in coefficient of drag for increasing Reynolds number. It was noted that this effect occurred at a higher Reynolds number for decreasing angle of attack, i.e., drag coefficient for 15 degrees showed little or no decrease for high Reynolds number.

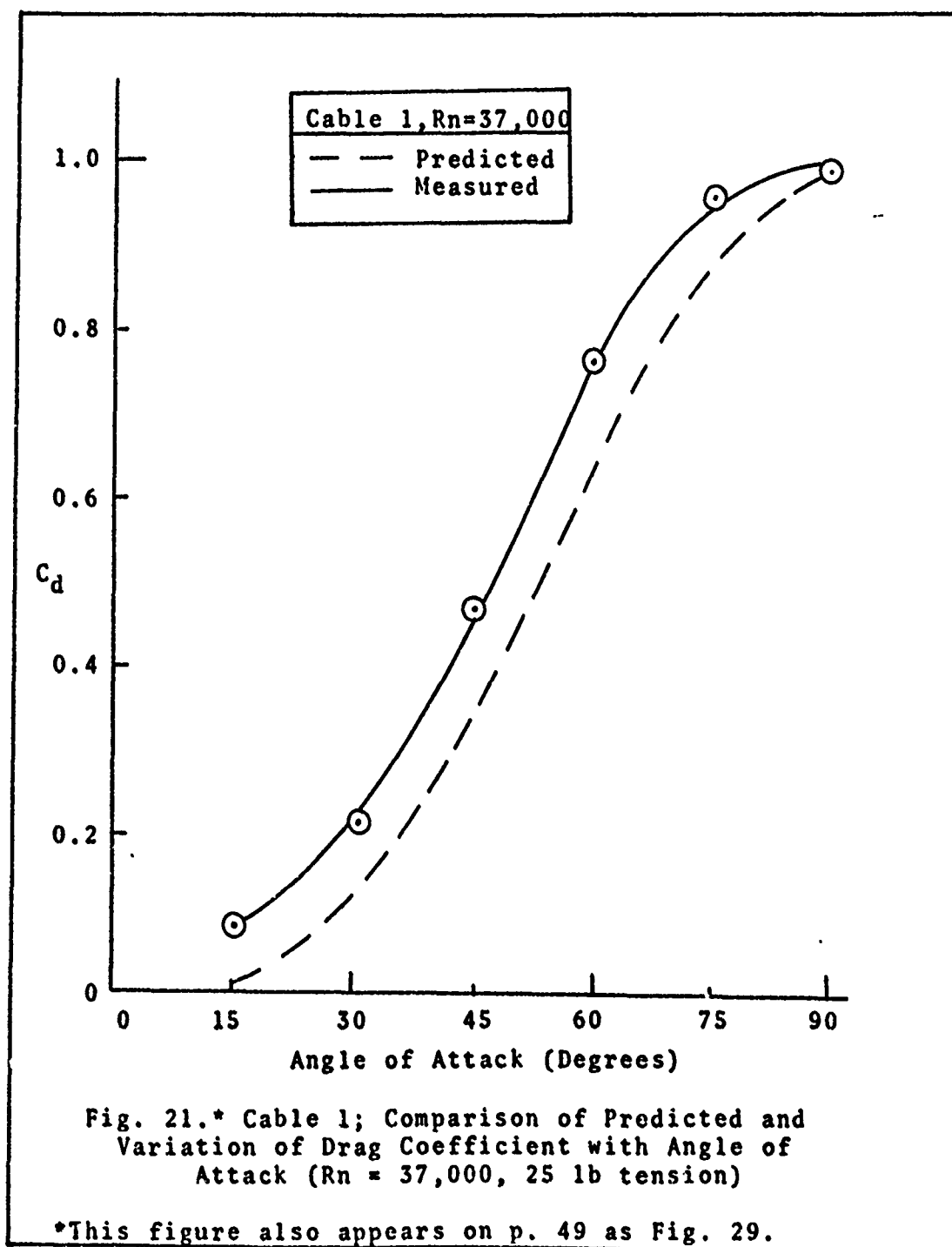
In Fig. 20, drag coefficient is plotted versus angle of attack with Reynolds number as parameter. The Reynolds number effect was seen more clearly here as the coefficient of drag decreased with increasing Reynolds number, the effect being most pronounced at high angles of attack.

It was found that the variation of drag coefficient with Reynolds number predicted by the Cross Flow Principle



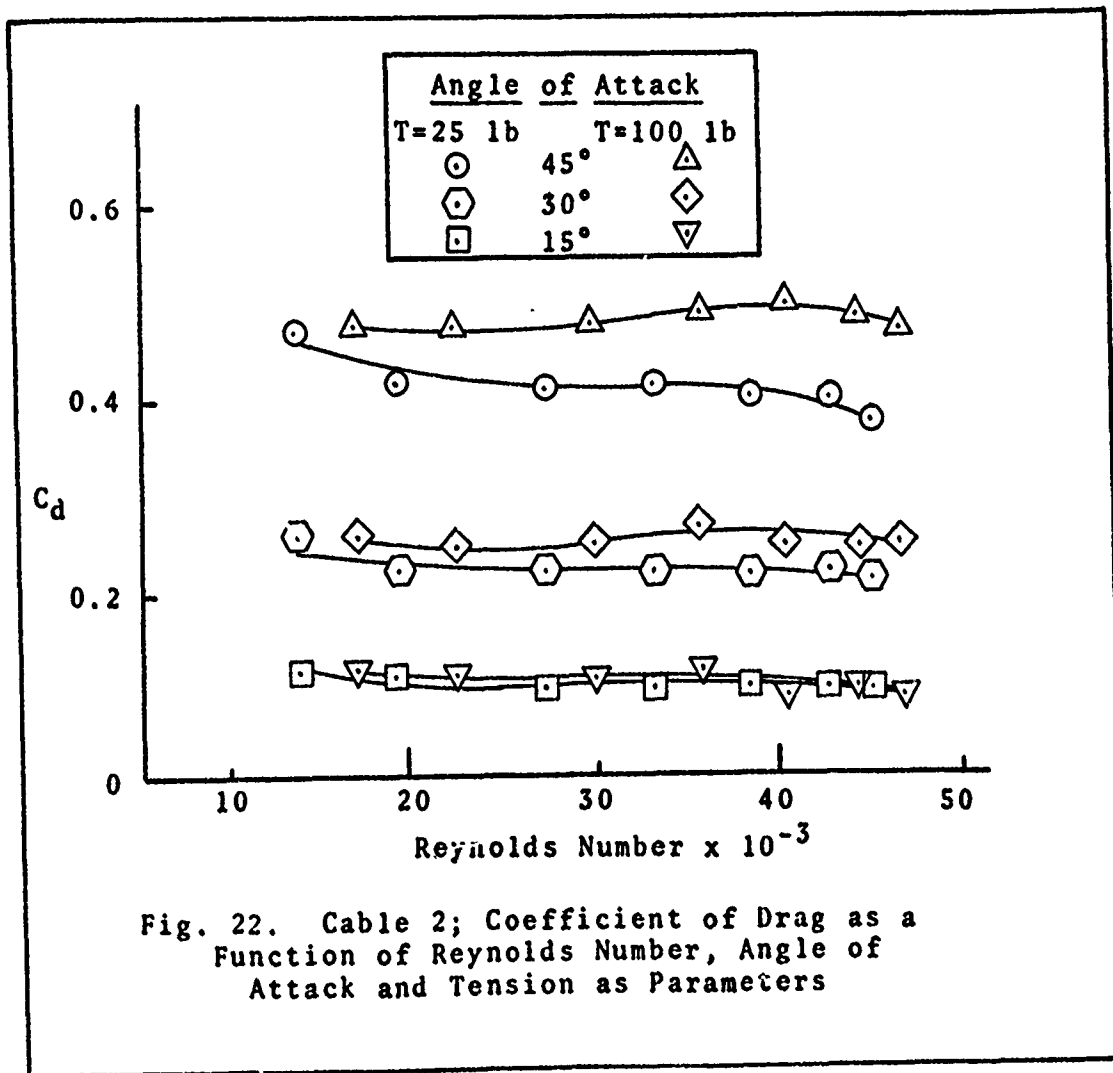


closely approximated the shape of the experimental curve, but the theoretical values of drag coefficient were consistently lower than experimental results, as shown in Fig. 21.



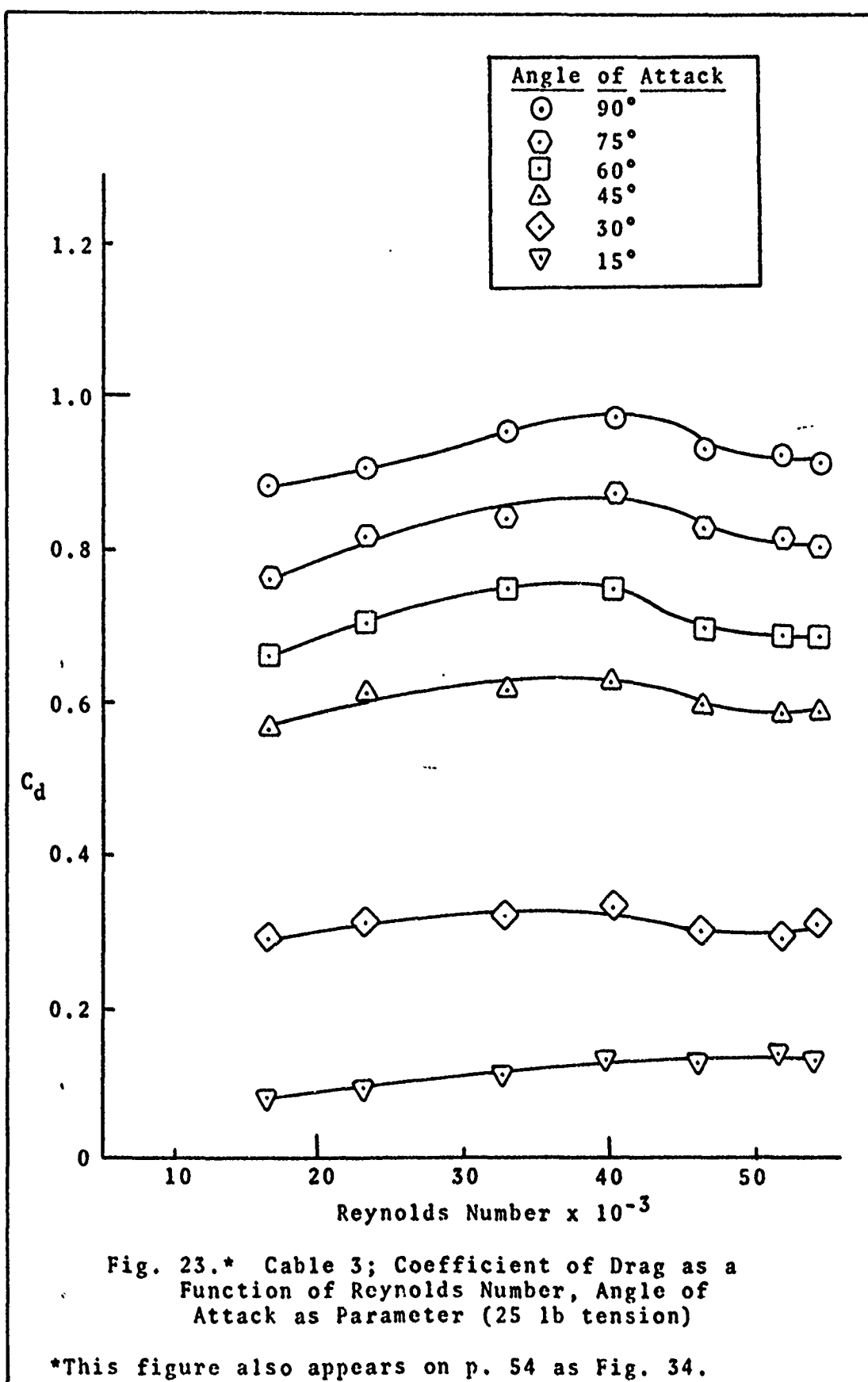
Cable 2. Cable 2 was tested over the Reynolds number range $R_n = 13,000-45,000$. The general results of testing were as found for Cable 1. The only major difference was that the coefficient of drag was consistently lower for Cable 2 (for corresponding angle of attack and Reynolds number) reaching a maximum of 1.1. Detailed results are provided in Figs. 30, 31, 32, and 33 in Appendix C.

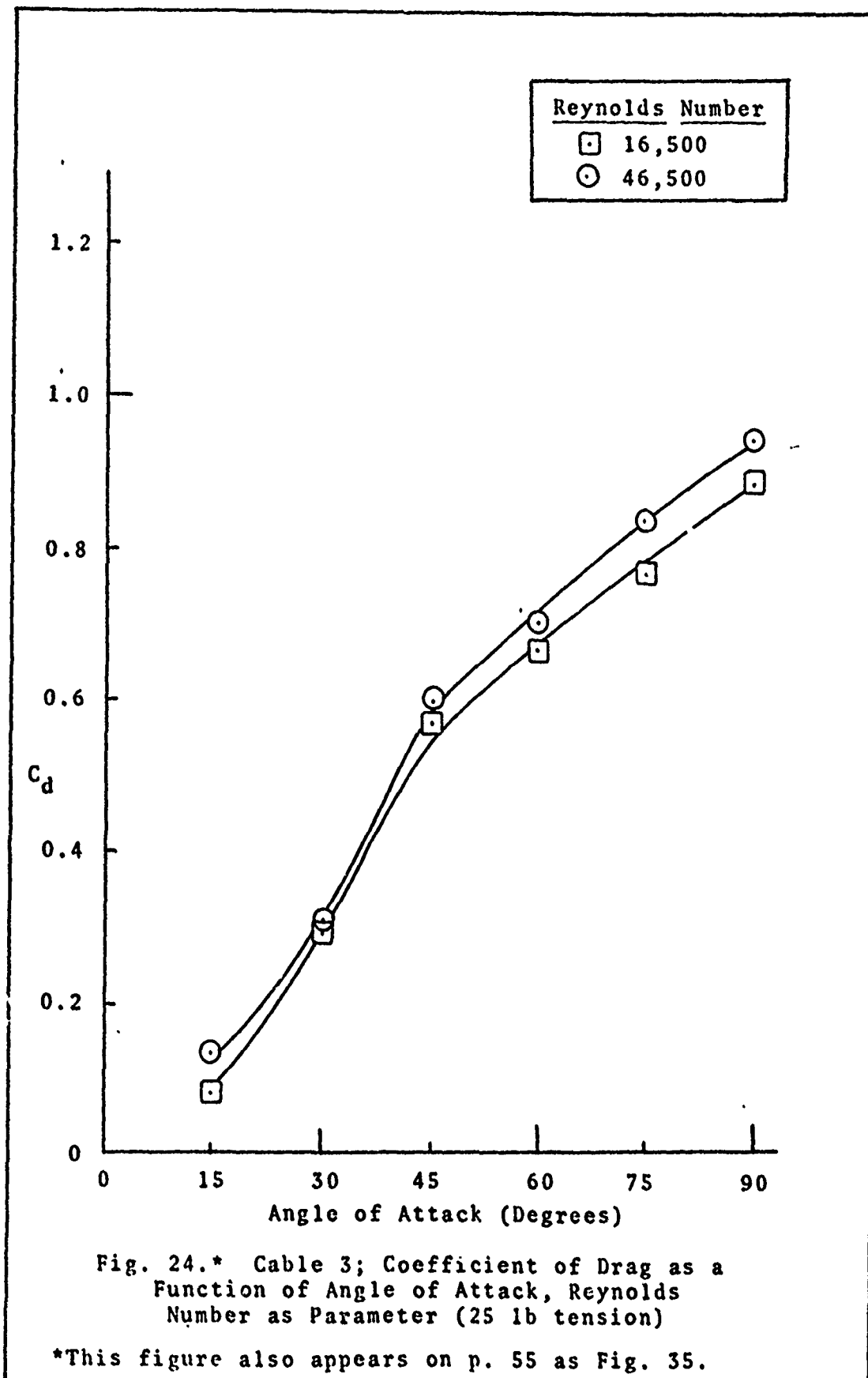
Drag coefficient was found to increase slightly under increased tension as shown below in Fig. 22.



Cable 3. Cable 3 was tested over the Reynolds number range $R_n = 18,000-55,000$. In general, all curves of drag coefficient versus Reynolds number exhibited a concave downward shape with no significant decrease in coefficient of drag at higher Reynolds numbers. The maximum coefficient of drag was slightly less than 1.0, and the curves were not consistently shaped as were those for Cables 1 and 2. See Fig. 23.

In Fig. 24, drag coefficient versus angle of attack is plotted with Reynolds number as parameter. It was seen here that coefficient of drag increased with Reynolds number; in addition, it was evident that the Cross Flow Principle would not predict the shape of this curve accurately.





Cable 4. Cable 4 was tested over the Reynolds number range $Rn = 18,000-48,000$. In general, Cable 4 exhibited characteristics similar to those of Cable 3. The major differences were (1) Cable 4 reached a maximum coefficient of drag slightly greater than 1.0 and (2) the curves of coefficient of drag versus Reynolds number were more similarly shaped and constant in nature. Coefficient of drag was a much more linear function of angle of attack for Cable 4 than predicted by the Cross Flow Principle. Figures 36 and 37, Appendix C, provide detailed results for Cable 4.

Test Apparatus. Although the Drag Frame gave reasonable results under the parameters presented in this study, it was found to be (1) inherently unstable when interfaced with the wire balance, (2) difficult to align due to its size and shape, (3) difficult to adjust and reconfigure due to the necessity of incorporating adjustment mechanisms into the frame, (4) too large, so that wind tunnel motor power limitations were imposed, and (5) limited in ability to test cables in the tension ranges encountered in actual practice.

Conclusions

Cables 1 and 2. In the range of Reynolds numbers tested (12,000 to 54,000), the results were in fair agreement with Schlichting (Ref 4:16) and Lindsey (Ref 3:171) for circular cylinders (a relatively constant coefficient of drag of 1.2 is predicted). Experimental results were in the neighborhood of 1.1 for Cable 1 and 1.0 for Cable 2, but these results were not constant over the test range.

Due to the shapes of the drag coefficient versus Reynolds number curves (concave up and decreasing at higher Reynolds numbers), it was concluded that the circular cables were approaching the critical Reynolds number range predicted by Fage and Warsap (Ref 4:459).

Although tension tests gave good results, it was concluded that more testing is necessary to establish trends.

Cables 3 and 4. The flat cables ($t/c = 1/2$) gave much higher coefficients of drag (1.0 as opposed to 0.6) than are predicted for elliptical cylinders of the same fineness ratio over the same test range (Ref 3:172). It was concluded that this variation could be attributed to (1) cable shape (basically rectangular), (2) roughness, and (3) other parameters, such as porosity.

It was concluded that critical Reynolds number effects were not noticeable for the flat cables, and that the Cross Flow Principle is not applicable to this type cable.

Test Apparatus. It was concluded that the Drag Frame is inadequate for further testing of cables except at very low tensions.

Summary

1. The curves of drag coefficient versus Reynolds number exhibited slightly concave upward shapes for the circular cables becoming distinctly concave downward in the critical Reynolds number range, and concave downward shapes for the flat cables.
2. Critical Reynolds number effects were noticeable for the circular cables, but were not noticeable for the flat cables.
3. The Cross Flow Principle predicted the general shape of the drag coefficient variation with angle of attack for the circular cables, but predicted a consistently low value of drag coefficient.
4. The Cross Flow Principle was not accurate for prediction of flat cable drag coefficients.
5. At low angles of attack, drag coefficient was relatively constant with Reynolds number for both circular and flat cables.

VI. Recommendations

It is recommended that:

1. Further testing on cable characteristics be carried out in a small diameter wind tunnel where side plates would not be necessary. This would facilitate high tension testing and ease of reconfiguration, as well as eliminate stability problems.
2. Parameters such as porosity and cable attitude (see p. 26) be considered for further testing.
3. Polynomial curves be fitted to the experimental data so that they can be incorporated into existing circling line dynamic analysis computer programs.
4. The lift characteristics of tow cables be investigated to determine their general nature, lift coefficient magnitudes, and the applicability of the Cross Flow Principle to lift coefficient prediction.
5. A theoretical analysis be made of the flow conditions around inclined cables, including the effects of extreme surface roughness, porosity, and cable tension. Predictions based upon this analysis could be compared to existing experimental data and might point out areas in which further wind tunnel testing might be used to advantage.

Bibliography

1. Dwinnell, James H. Principles of Aerodynamics. New York: McGraw-Hill Book Co., 1949.
2. Liller, James H. Analysis of the Dynamic Motion of a Circling Line in the Presence of Winds and Gusts. Unpublished Thesis. Wright-Patterson AFB, Ohio: Air Force Institute of Technology, 1969.
3. Lindsey, W. F. Drag of Cylinders of Simple Shapes. NACA Technical Report 619. Langley Field, Virginia: Langley Memorial Aeronautical Laboratory, 1937.
4. Schlichting, Hermann. Boundary Layer Theory. New York: McGraw-Hill Book Co., 1955.
5. Simons, John C. and B. C. Dixon. Long-Line Loiter: Improvement of Some Free-Fall and Circling-Line Techniques. ASD-TR-69-65 (Vol. I). Wright-Patterson AFB, Ohio: Aeronautical Systems Division, 1969.

Appendix A

Cross Flow Principle

The Cross Flow Principle holds that the airflow pattern and hence the dynamic pressure acting on an inclined cylinder is a function of the airflow component normal to the cylindrical axis.

Consider a circular cylinder of length l and diameter d and having "proper" drag coefficient (drag coefficient based on total wetted cross sectional area) $C_{d\pi}$. Let this cylinder be inclined at angle of attack α to a uniform airstream of velocity V as shown in Fig. 25.

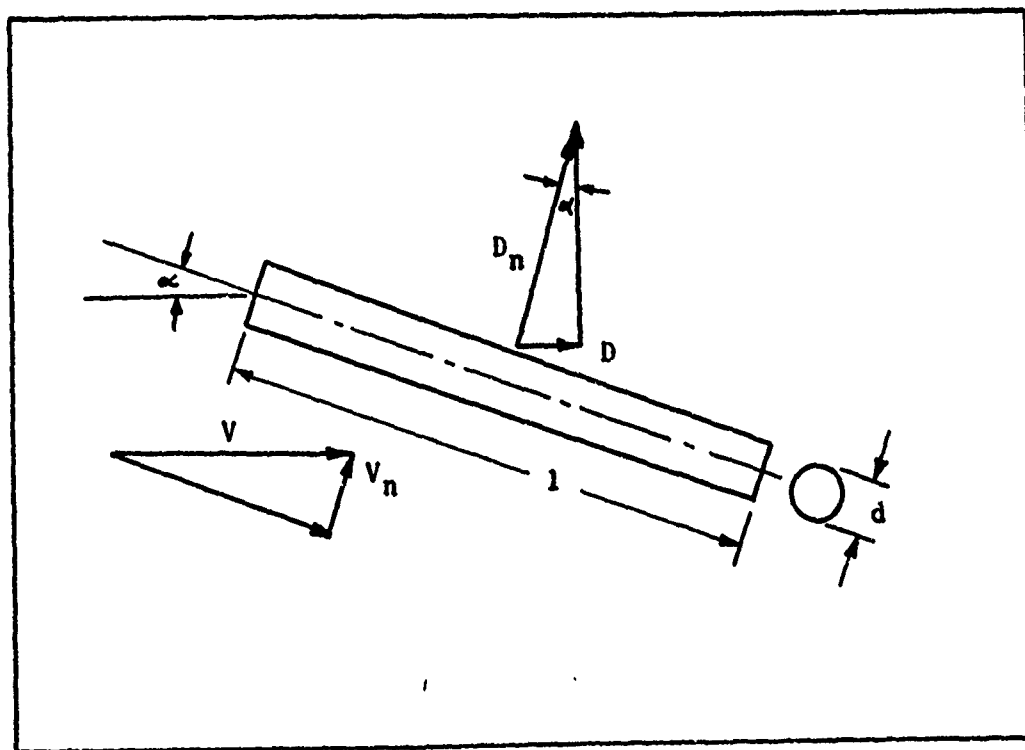


Fig. 25. Inclined Circular Cylinder in Airstream

From the geometry of Fig. 25, the component of flow normal to the cylindrical axis is

$$V_n = V \sin \alpha \quad (1)$$

where V_n = "normal" airstream velocity

V = airstream velocity

α = cylinder angle of attack

The "normal" drag force acting on the inclined cylinder is

$$D_n = C_{d\pi} q_n S_\pi = C_{d\pi} (1/2 \rho V_n^2) d l \quad (2)$$

where D_n = "normal" drag force

C_d = drag coefficient based on "proper" area

q_n = "normal" dynamic pressure

S_π = "proper" cross sectional area

ρ = airstream density

d = cylinder diameter

l = cylinder length

Substituting Eq (1),

$$D_n = C_{d\pi} (1/2 \rho V^2) \sin^2 \alpha d l \quad (3)$$

The component of this "normal" drag force in the direction of the airstream is

$$D = D_n \sin \alpha = C_{d\pi} (1/2 \rho V^2) d l \sin^3 \alpha \quad (4)$$

where D = drag force parallel to airflow direction.

If, however, the drag coefficient (based on "proper" area) of the inclined cylinder is defined by

$$D = C_d (1/2 \rho V^2) d l \quad (5)$$

where C_d = drag coefficient of cylinder at angle of attack, then since the drag forces expressed by Eqs (4) and (5) are equal (i.e., both express the magnitude of the drag force acting on the cylinder in the direction of the free airstream),

$$C_d = C_{d\pi} \sin^3 \alpha \quad (6)$$

From Eq (6), it can be seen that the Cross Flow Principle predicts the "proper" drag coefficient of an inclined circular cylinder to be equal to the "proper" drag coefficient at 90 degrees angle of attack multiplied by the cube of the sine of the cylinder angle of attack.

Appendix B

Data ReductionTest Atmospheric Conditions

Temperature and pressure were recorded before and after each test run to determine average test conditions; pressures were corrected for temperature before averaging.

Atmospheric density was corrected for temperature and pressure by

$$\rho = \rho_o \left(\frac{P}{P_o} \right) \left(\frac{T_o}{T} \right) \quad (7)$$

where $\rho_o = 0.002378$ slugs per ft³

$P_o = 29.92$ in. of mercury

$T_o = 518.6$ degrees Rankine

Atmospheric viscosity was corrected for temperature by the following (Ref 1:15):

$$\mu = (338.5 + 0.575 T) \times 10^{-9} \quad (8)$$

where μ = dynamic viscosity in pound seconds per ft²

T = temperature in degrees Fahrenheit

Drag Coefficient Reference Area

The reference area used for all drag coefficients was the "proper" cross sectional area, the total wetted cable cross sectional area encountered by the air stream:

$$A = \frac{18 t}{\sin \alpha} \quad (9)$$

where A = "proper" cable cross sectional area

t = cable thickness normal to airstream

The appropriate dimensions for a flat cable are shown below.

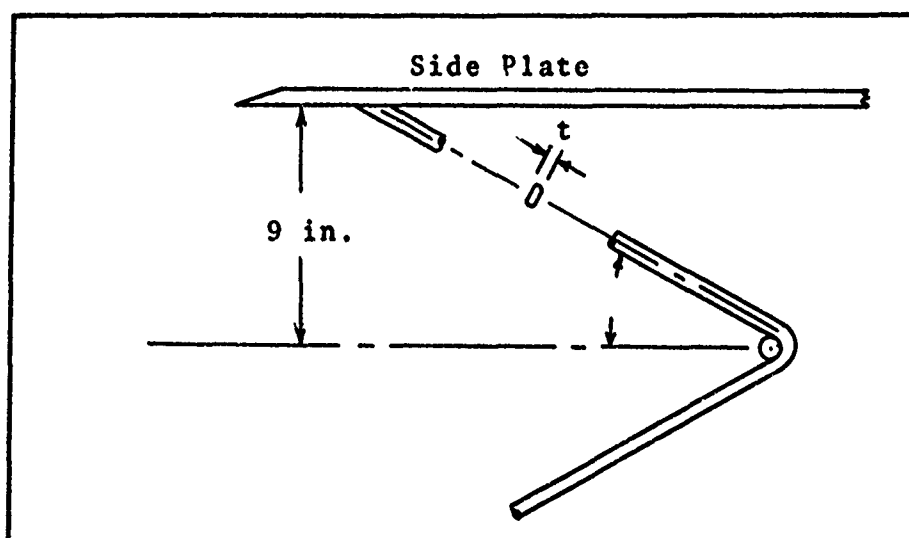


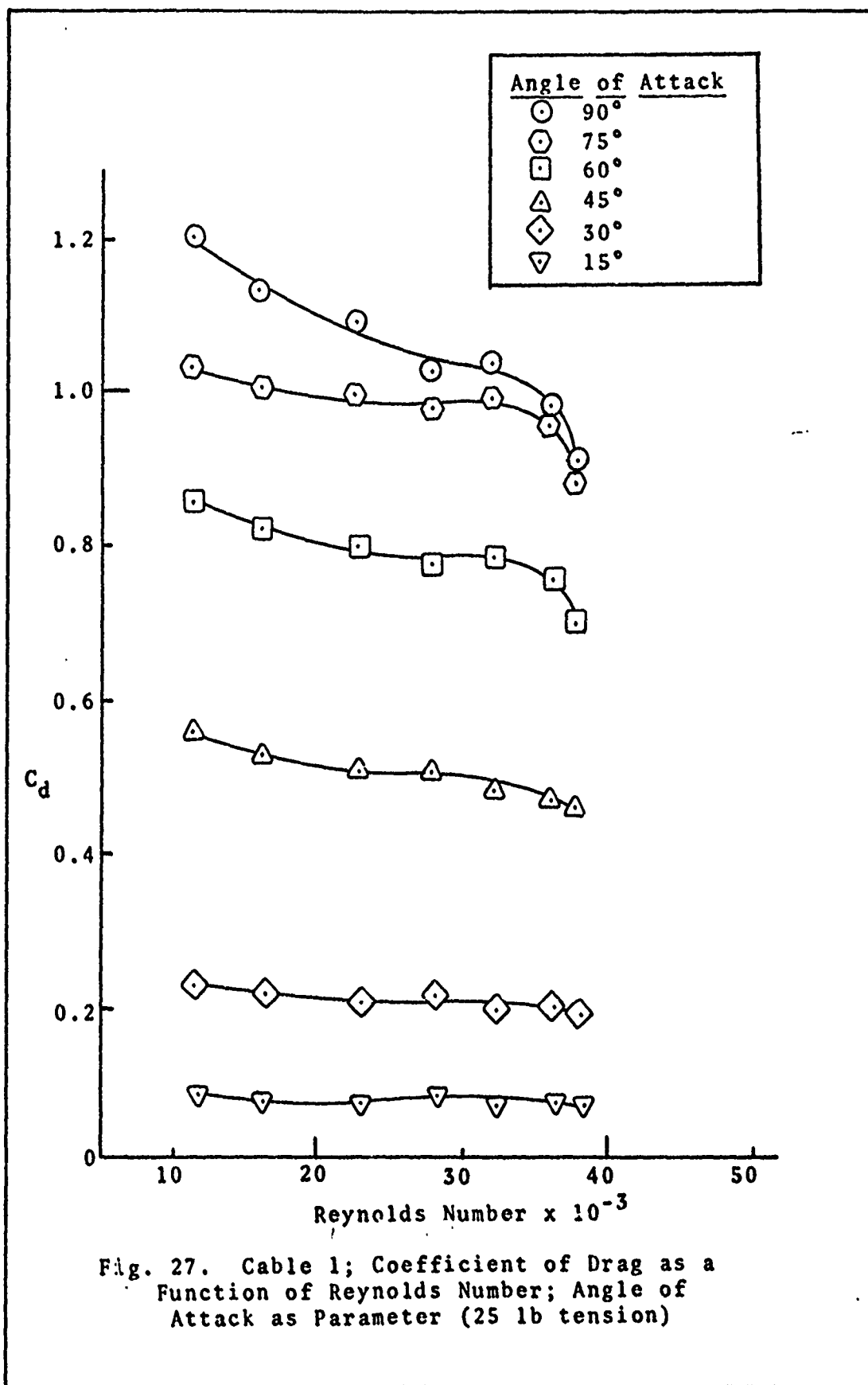
Fig. 26. "Proper" Cross Sectional Area (For a Flat Cable)

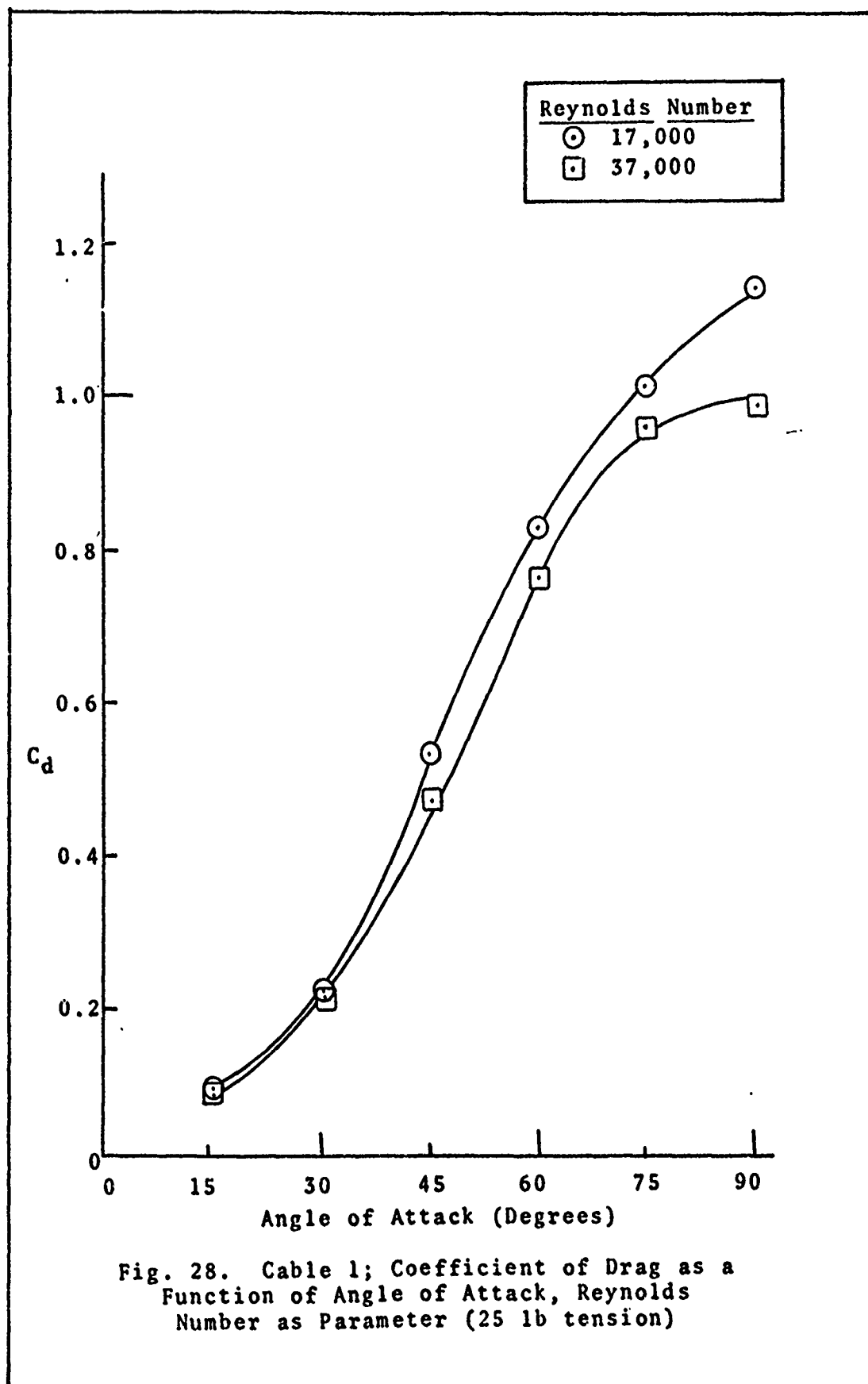
Reynolds Number Characteristic Length

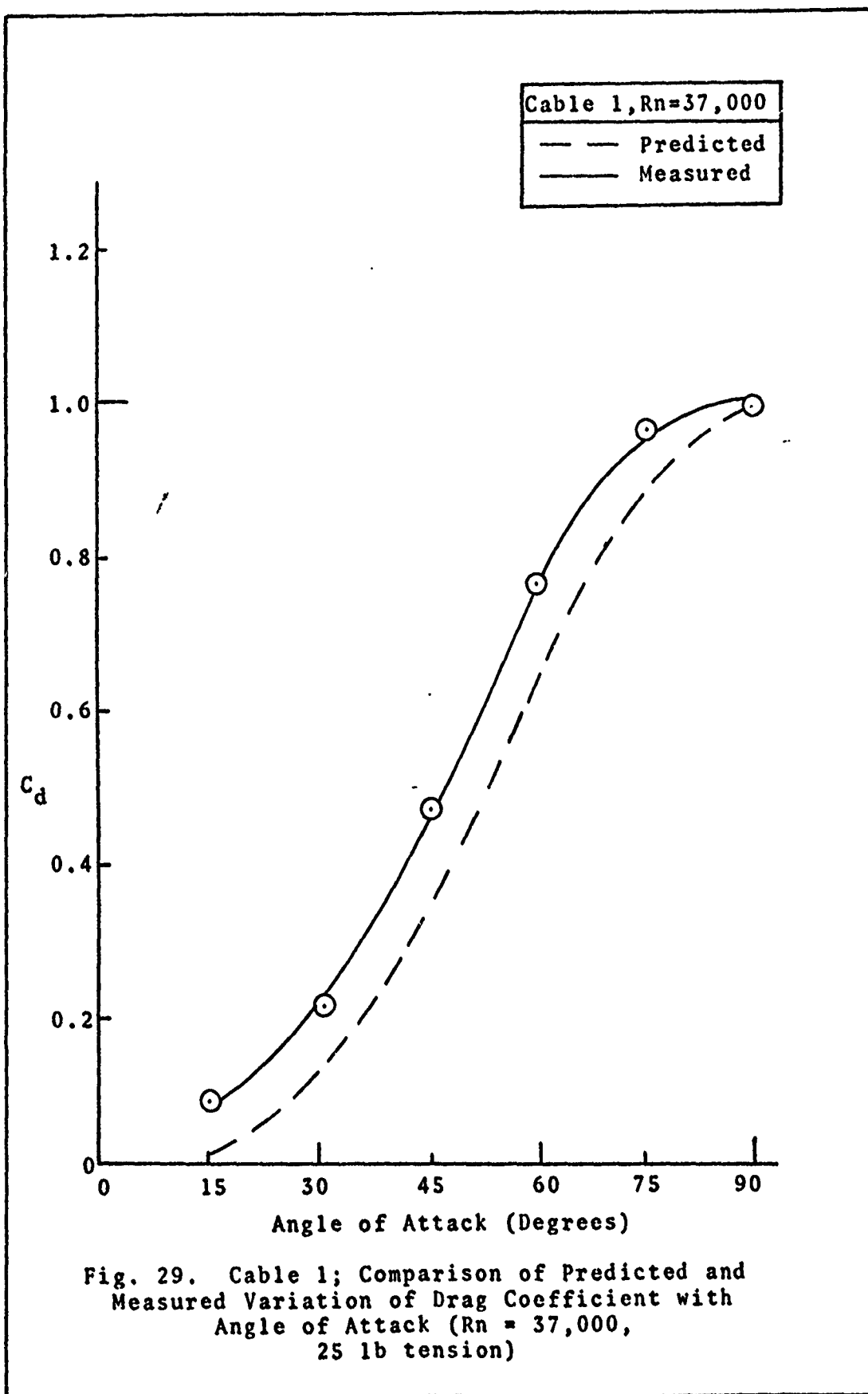
The characteristic length used for calculation of all Reynolds numbers was the cable cross sectional dimension parallel to the airstream when the cable was at 90 degrees angle of attack. (In the case of the two "flat" cables, this length was either 3/8-inch or 1/2-inch.)

Appendix C

Graphical Results of
Cable Drag Test Program







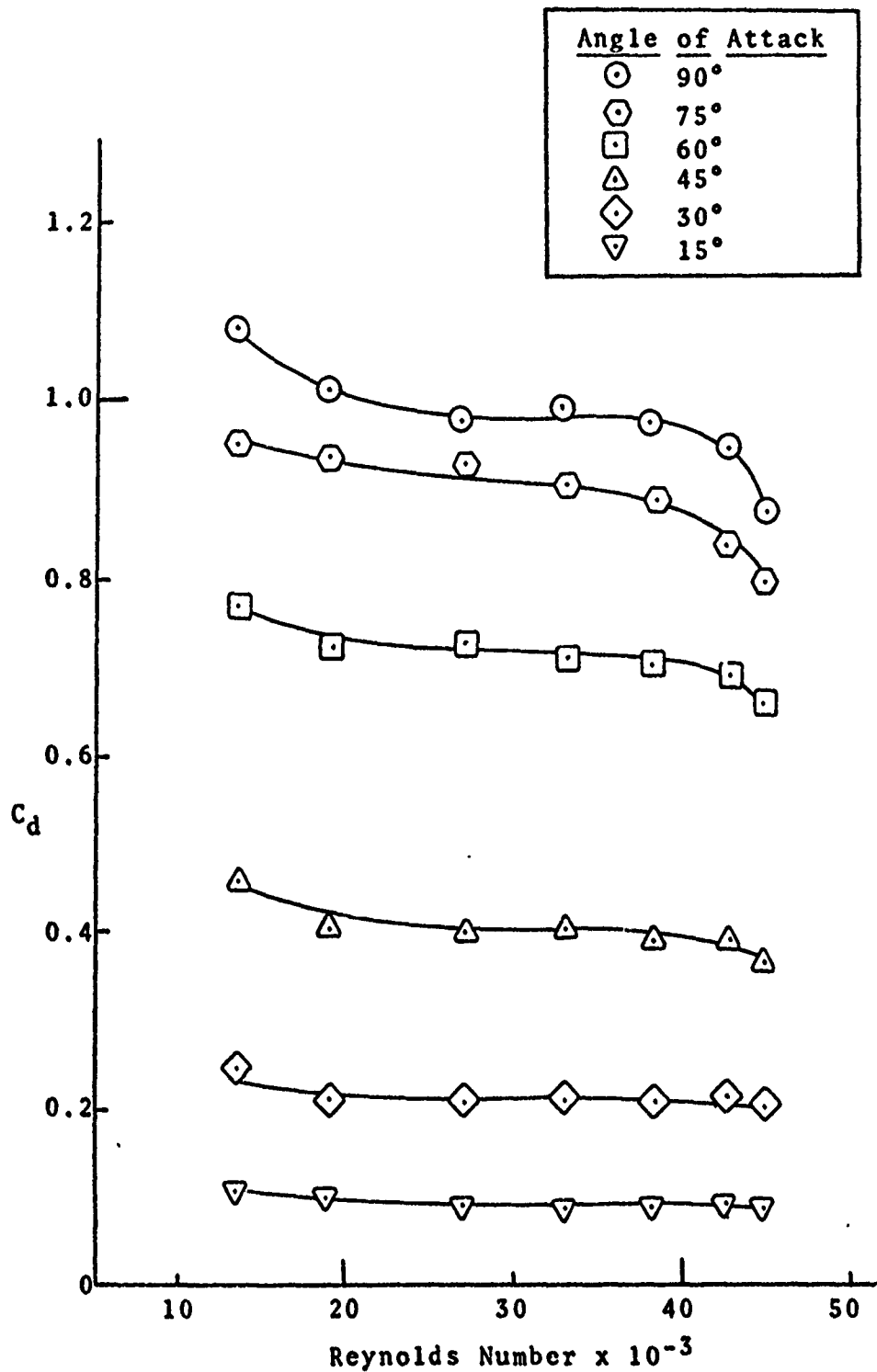
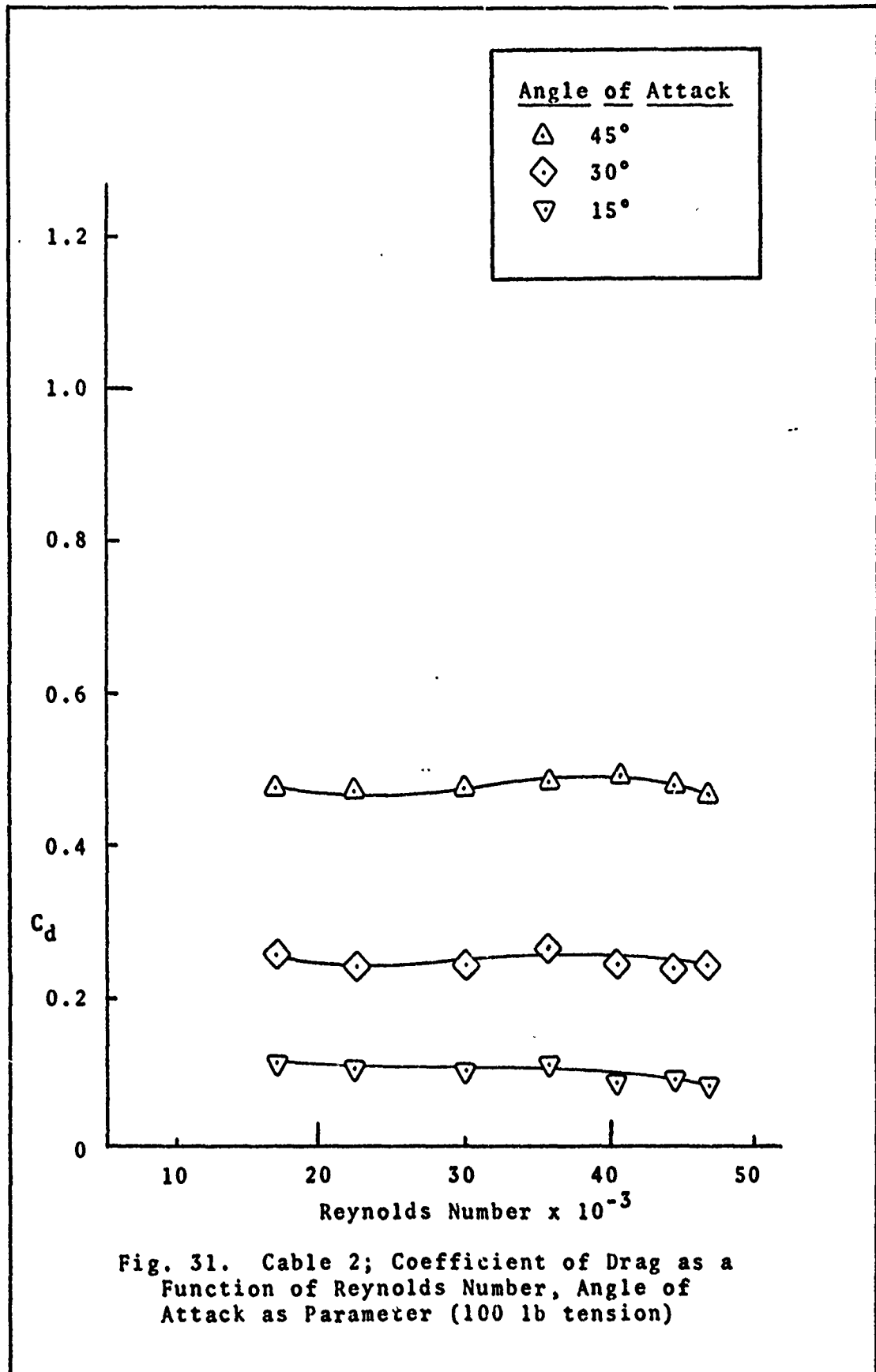
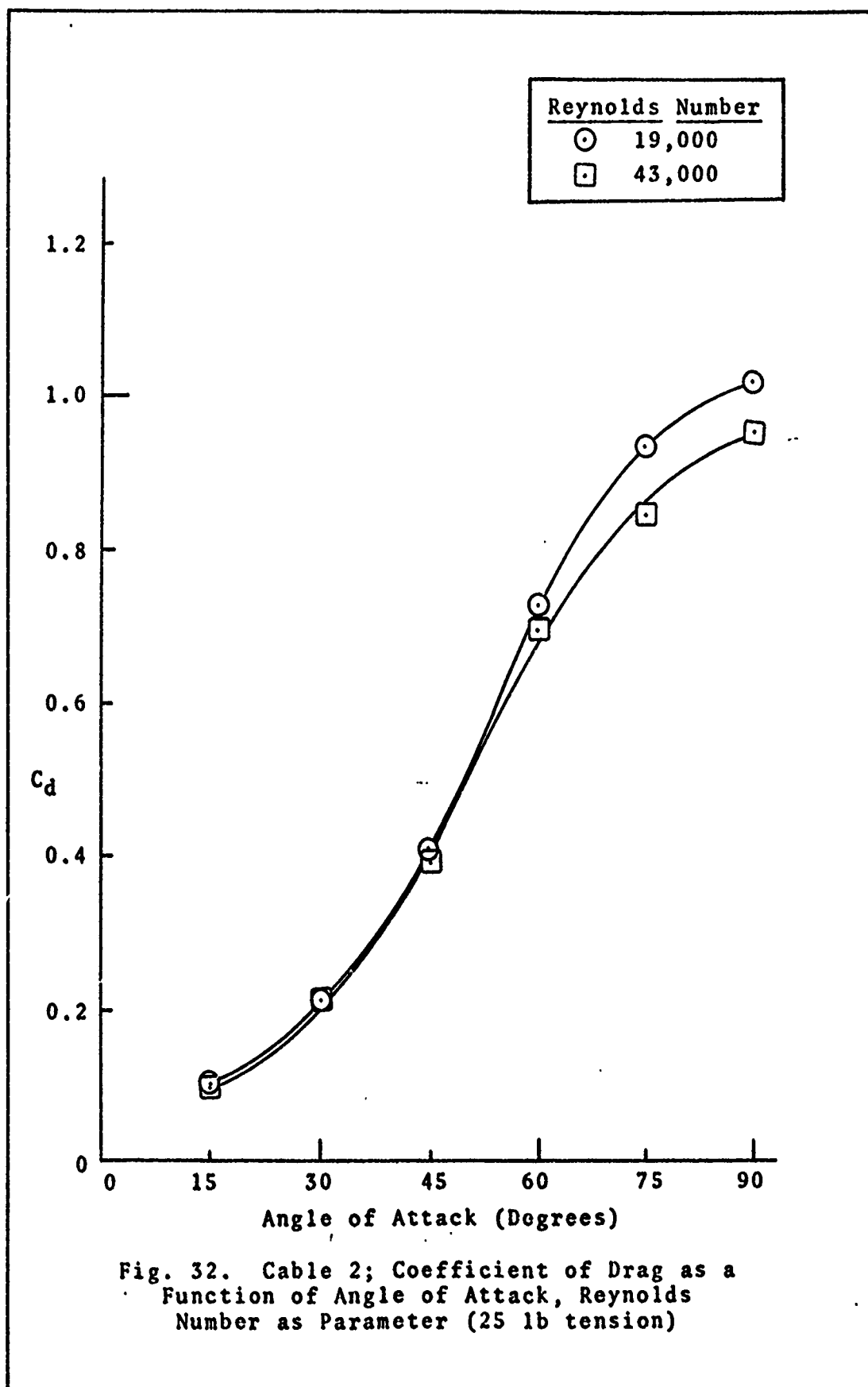
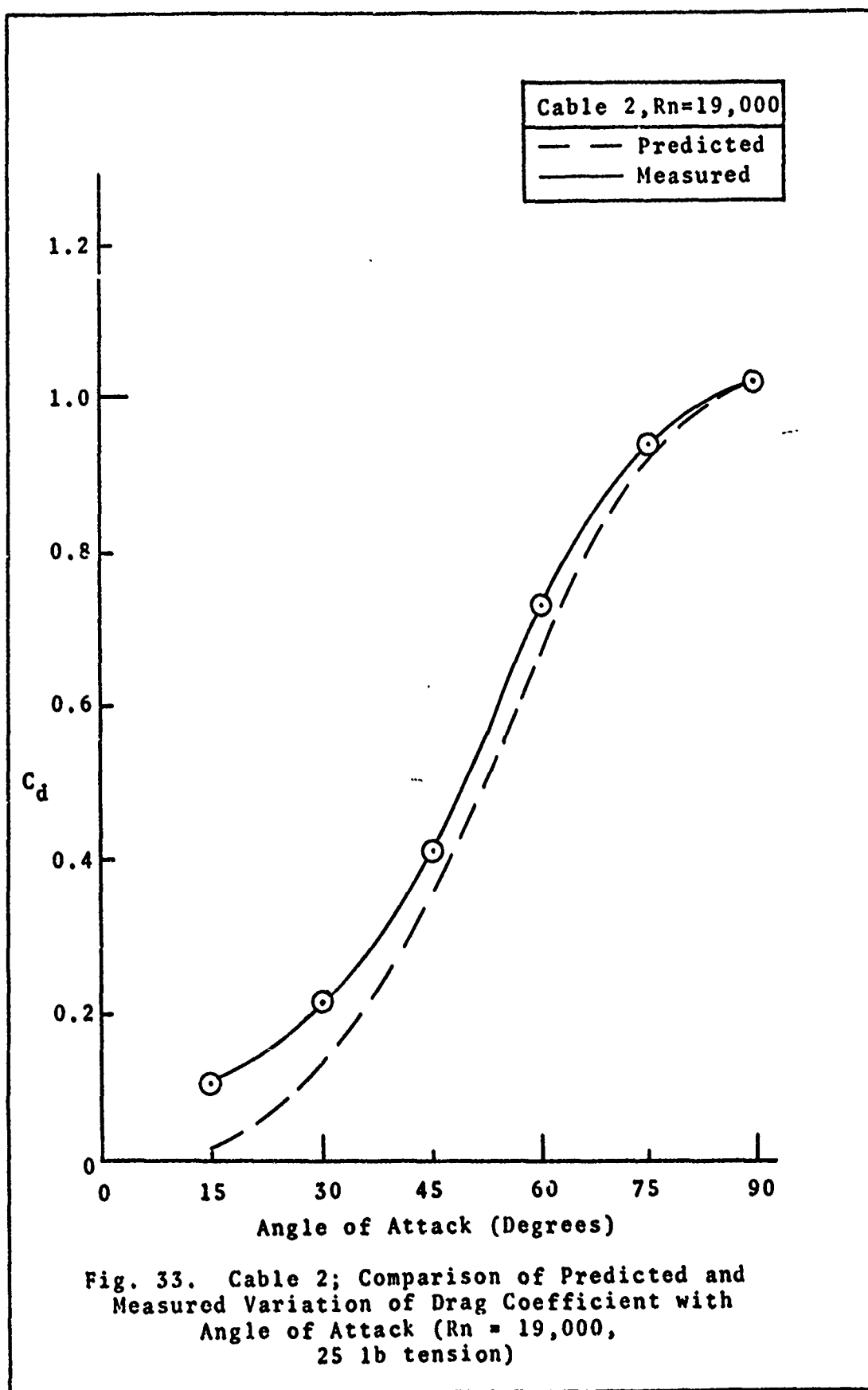
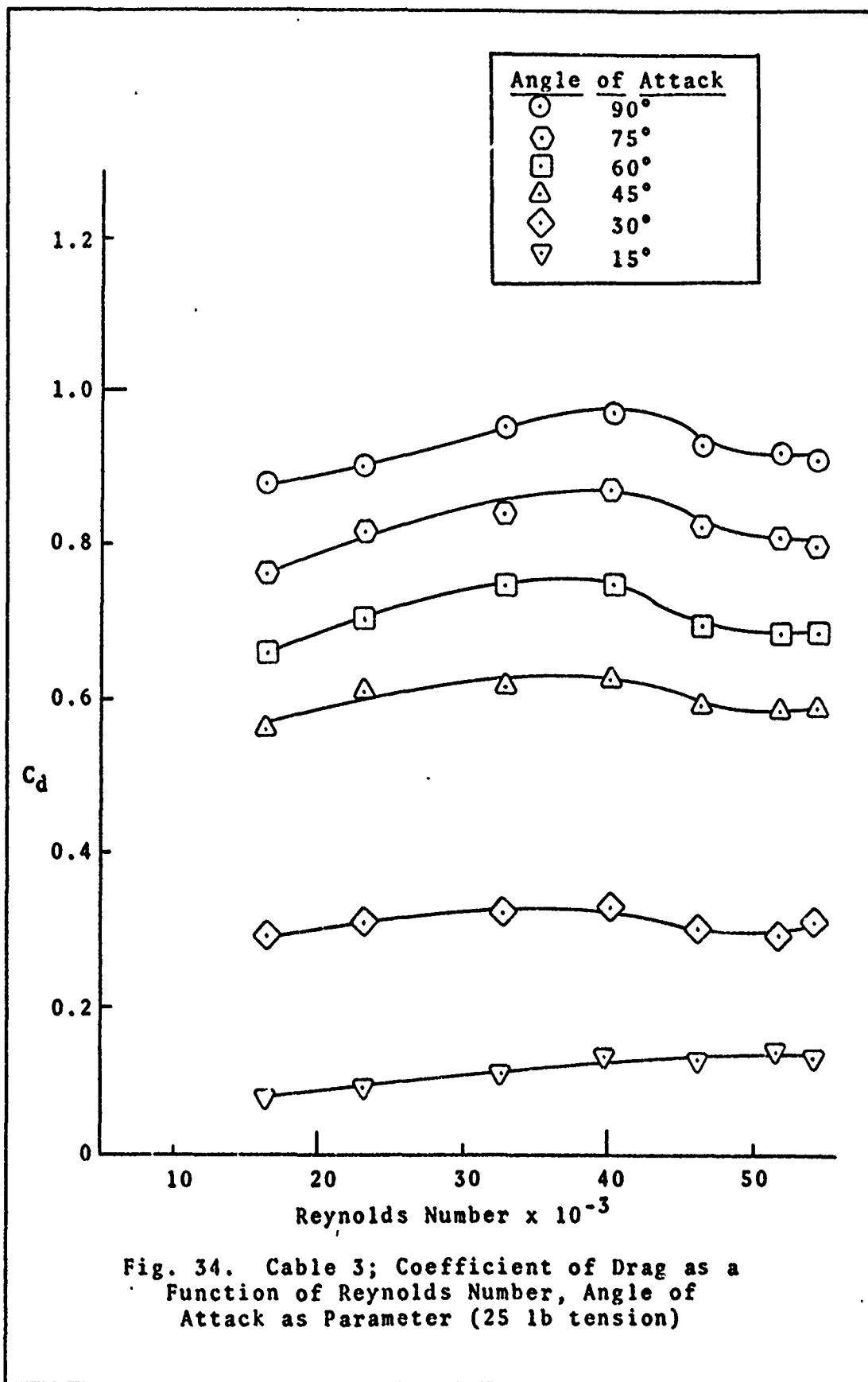


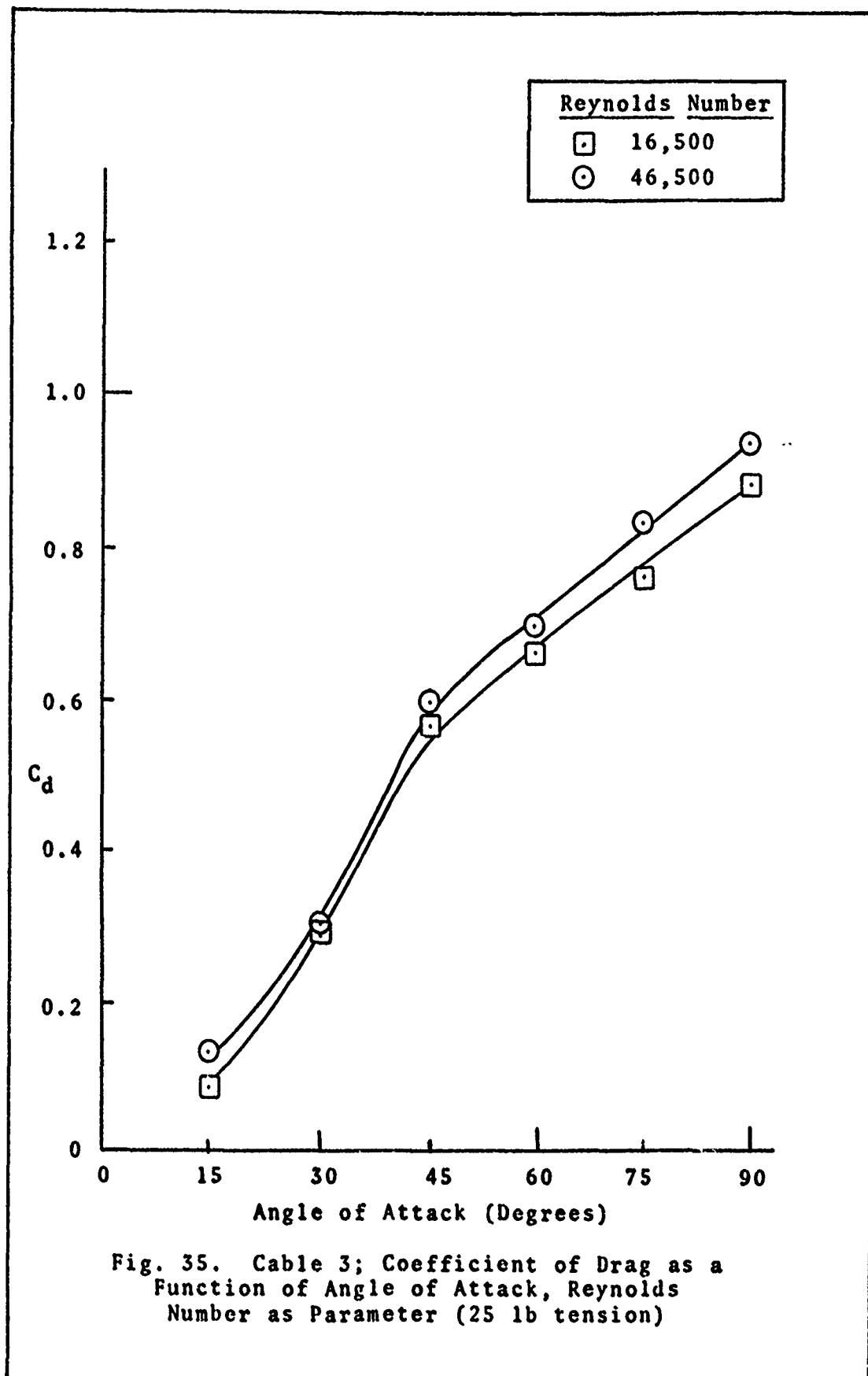
Fig. 30. Cable 2; Coefficient of Drag as a Function of Reynolds Number, Angle of Attack as Parameter (25 lb tension)











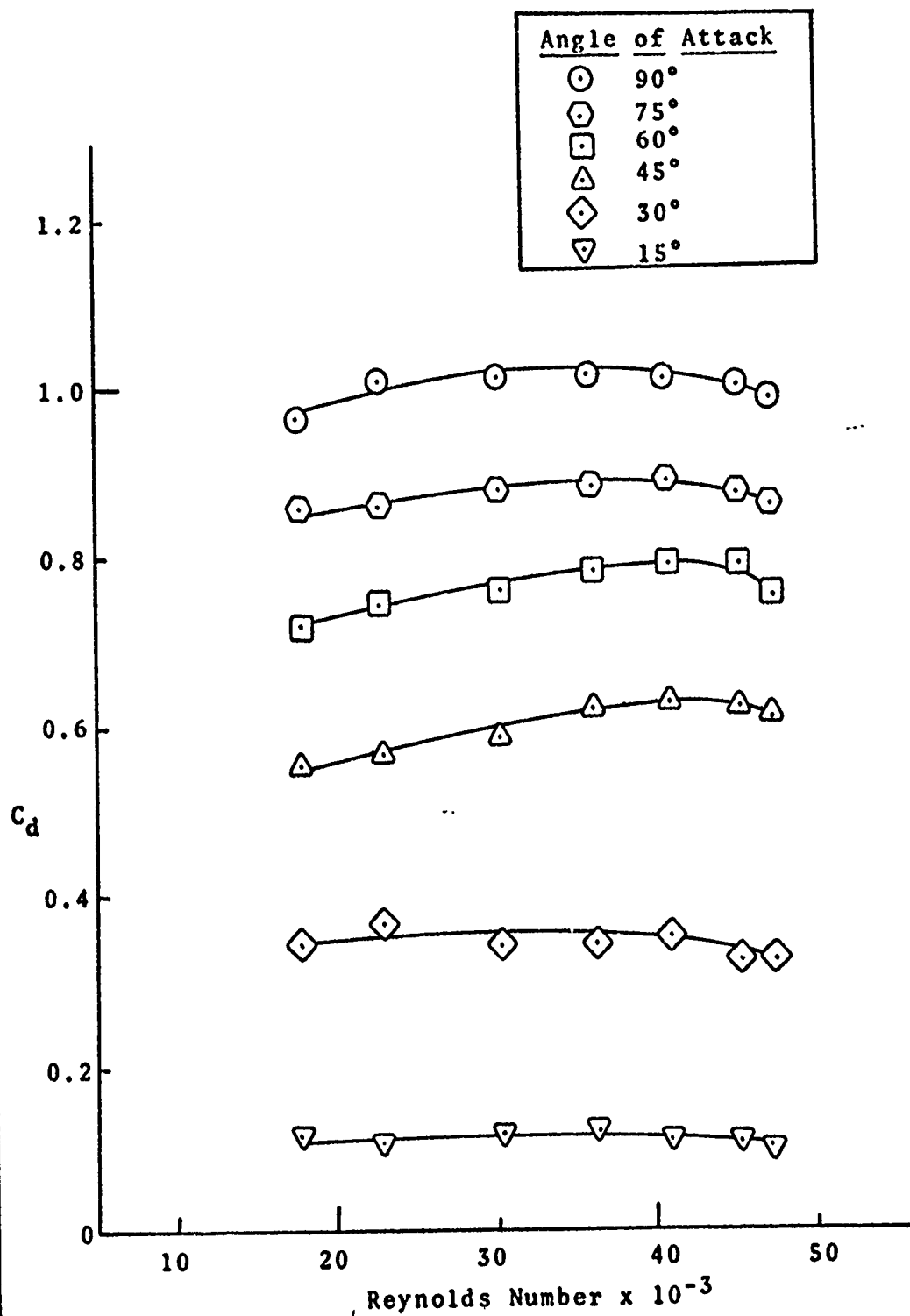
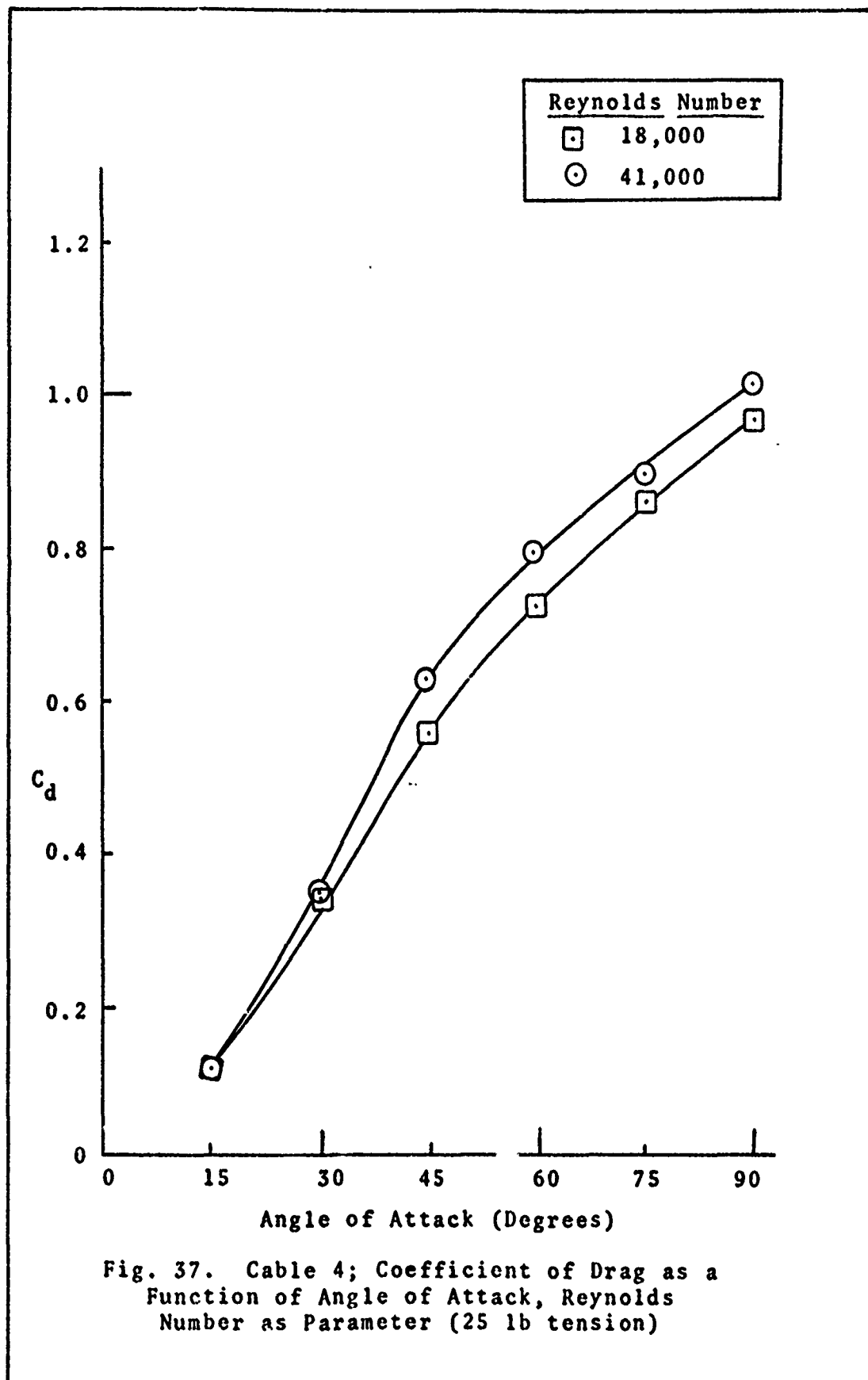


Fig. 36. Cable 4; Coefficient of Drag as a Function of Reynolds Number, Angle of Attack as Parameter (25 lb tension)



Vita

Burdette James Barnes, Jr. was born on 19 April 1938 in San Luis Obispo, California. He was graduated from Arcata Union High School in Arcata, California in 1956 and attended Humboldt State College in Arcata until joining the United States Air Force in 1958. In 1962, he entered the Airman Education Commission Program at the University of Oklahoma, was graduated with the degree of Bachelor of Science in Aerospace Engineering in 1965, and entered the Air Force Officer Training School in March 1965. He received his commission in May 1965 and served as a Missile Launch Control Officer (Titan II) until May 1969. In June 1969, he entered the Air Force Institute of Technology from which he obtained the degree of Master of Science in Astronautical Engineering in June 1971.

Permanent Address: 122 13th Street

Arcata, California 95521

Vita

John L. Pothier was born in Jacksonville, Florida on 20 May 1942. He was graduated from Ada High School, Ada, Ohio in May 1969 and earned the degree of Bachelor of Science in Aerospace Engineering from the University of Cincinnati in June 1964. He was commissioned in the United States Air Force through the AFROTC program in July 1964, attended the Missile Officer course at Chanute AFB, Illinois, and served three years as a Minuteman II Targeting/Alignment Team Chief at Grand Forks AFB, North Dakota. In 1967, he was assigned to the Guidance and Control Engineering Branch, SAMSO Minuteman System Program Office. In June 1969, he entered the Air Force Institute of Technology from which he obtained the Degree of Master of Science in Astronautical Engineering in June 1971.

Permanent Address: 7071 Bobhird Drive
San Diego, California 92119

This thesis was typed by Mrs. Jane Manemann.